CEEDO-TR-78-30

LEVEL II (2)

THE EVAPORATION AND DISPERSION OF HYDRAZINE PROPELLANTS FROM GROUND SPILLS

GERHARD ILLE
DIRECTORATE OF ENVIRONICS
ENVIRONMENTAL ASSESSMENT RESEARCH DIVISION

CHARLES SPRINGER
UNIVERSITY OF ARKANSAS

AUGUST 1978

FINAL REPORT FOR PERIOD JULY 1977 - JULY 1978

CEEDO

CIVIL AND ENVIRONMENTAL ENGINEERING DEVELOPMENT OFFICE
(AIR FORCE SYSTEMS COMMAND)
TYNDALL AIR FORCE BASE
FLORIDA 32401

UNCLASSIFIED

SECURITY CLASSIFICATION OF THIS PAGE (When Data Entered)

REPORT DOCUMENTATION PAGE

READ INSTRUCTIONS BEFORE COMPLETING FORM

1. REPORT NUMBER: CEEDO-TR-78-30	2. GOVT ACCESSION NO.
3. RECIPIENT'S CATALOG NUMBER	
4. TITLE (and Subtitle): The Evaporation & Dispersion of Hydrazine Propellants from Ground Spills	5. TYPE OF REPORT & PERIOD COVERED: Final Jul 1977-Jul 1978
6. PERFORMING ORG. REPORT NUMBER	
7. AUTHOR(s): Gerhard Ille, Charles Springer, University of Arkansas	8. CONTRACT OR GRANT NUMBER(s): AUJ
9. PERFORMING ORGANIZATION NAME AND ADDRESS: Det 1 ADTC/ECA, Tyndall AFB FL 32403	10. PROGRAM ELEMENT, PROJECT, TASK AREA & WORK UNIT NUMBERS: Program Element - 62601F, Project - 1900, Task - 5A, Work Unit - 35
11. CONTROLLING OFFICE NAME AND ADDRESS: Det 1 ADTC/ECA, Tyndall AFB FL 32403	12. REPORT DATE: July 1978
	13. NUMBER OF PAGES: 93
14. MONITORING AGENCY NAME & ADDRESS (if different from Controlling Office)	15. SECURITY CLASS. (of this report): UNCLASSIFIED
	15a. DECLASSIFICATION/DOWNGRADING SCHEDULE

16. DISTRIBUTION STATEMENT (of this Report)

Approved for public release, distribution unlimited.

17. DISTRIBUTION STATEMENT (of the abstract entered in Block 20, if different from Report)

18. SUPPLEMENTARY NOTES

19. KEY WORDS (Continue on reverse side if necessary and identify by block number)

Dispersion Modeling
Air Quality
Evaporation
Ground Spills
Gaussian Model
Environmental Quality
Environics

20. ABSTRACT (Continue on reverse side if necessary and identify by block number)

A propellant evaporation and dispersion model has been developed for hydrazine ground spills. The evaporation algorithm computes the rate of evaporation as a function of soil temperature, solar insolation, air temperature, wind velocity and spill dimensions. The single source Gaussian dispersion portion calculates the downwind, ground-level centerline concentration based on dispersion coefficients available in current EPA models. The dispersion algorithm also computes the crosswind dimension of a hazard corridor defined by the Short Term Public Limit (STPL) or other selected concentrations. (Reference 8).

DD FORM 1 JAN 73 1473 EDITION OF 1 NOV 65 IS OBSOLETE

UNCLASSIFIED

SECURITY CLASSIFICATION OF THIS PAGE (When Data Entered)

78 09 29 001

393 250

20. Abstract (continued)

Evaporation rates are calculated for 200, 20,000 and 36,000 liter N_2H_4, MMH and UDMH spills. Downwind peak concentration levels were calculated for each spill size for ambient air temperatures of 0, 15 and 30°C. Sensitivity analyses were performed for the evaporation input parameters to determine qualitatively the measurement accuracy required. Finally, hazard corridors, defined by the Short-Term Public Limit (STPL) concentration, were computed for N_2H_4, MMH and UDMH evaporating for the above spill sizes at 15°C ambient temperature.

PREFACE

This report was prepared by the Air Force Civil and Environmental Engineering Development Office under Job Order Number 19005A35. It documents the work completed between July 1976 and July 1978. Dr Charles Springer, University of Arkansas, and Capt Gerhard Ille were the principal investigators.

The authors wish to thank Major Peter S. Daley, Major Joseph B. Hooten, Major Michael G. MacNaughton, Captain Harvey Clewell, and AIC John C. Dobbins for their assistance and contributions. Special thanks go to Capt Dennis F. Naugle, Chief, Environmental Modeling Branch, for his invaluable guidance and contributions to this study and report preparation.

This report has been reviewed by the Information Officer (IO) and is releasable to the National Technical Information Service (NTIS). At NTIS, it will be available to the general public, including foreign nations.

This report is approved for publication.

CHARLES SPRINGER, PhD
Professor, Department of
Chemical Engineering
University of Arkansas

GERHARD ILLE, Capt, USAF, BSC
Project Officer
Environmental Assessment
Research Division

PETER A. CROWLEY, Maj, USAF, BSC
Director of Environics

JOSEPH S. PIZZUTO, Col, USAF, BSC
Commander

(The reverse side of this page is blank)

TABLE OF CONTENTS

LIST OF FIGURES

LIST OF FIGURES (Concluded)

LIST OF TABLES

SECTION I

INTRODUCTION

1. Increased AF use of hydrazine propellants and more stringent Occupational Safety and Health Administration (OSHA) and Environmental Protection Agency (EPA) regulations have greatly increased the need to predict concentrations of polluting chemicals discharged into the environment. In January 1976 the AF Space and Missile Systems Organization (SAMSO) identified Technology Need (TN-SAMSO-CEEDO-2109-76-45) that addressed this issue. The TN specifically stated that "The fate of the hydrazine fuels entering the environment is insufficiently characterized" (Reference 1). Prediction techniques available at missile sites prior to this study were not easily adaptable because they required temperature difference input data not commonly available and because photochemical reactions and atmospheric decomposition were not considered.

2. Hydrazine propellants are used in a variety of systems, such as space launch vehicles, strategic missiles and satellites and the F-16 Emergency Power Unit. The environmental impact of hazardous chemicals vented into the atmosphere or accidentally spilled during loading and off-loading operations can be more quickly elucidated through use of computerized evaporation and dispersion analysis techniques. These predictive techniques are crucial to assessing the hazard hydrazines may pose to man.

3. The objective of this technical report is to present a technique for computing evaporation rates from accidental spills and to illustrate how a simple physical dispersion model can be used to make air quality predictions downwind from the spill. This report assumes the evaporation from a non-porous, non-absorbing, flat surface and does not address atmospheric chemical reactions of the evaporating propellant. In addition, the evaporation model pertains strictly to pure missile propellants and cannot be applied straight forwardly to mixtures, such as used in TITAN missiles and the F-16 aircraft. The model is currently being modified to handle propellant mixtures.

The computation of evaporation rates and downwind concentrations are important since they have a major bearing on the size of the hazard corridor that must be evacuated to protect the populace from the spill. Example hazard corridor computations for drum, trailer and railcar propellant spills are illustrated in Section IV.

4. A number of dispersion models were reviewed to determine which was most applicable to the propellant problem. They include the box model commonly used for urban area sources, the Gaussian plume model widely

used for continuous elevated and ground sources, the Gaussian puff model used for instantaneous explosive sources and the empirical temperature difference model used at the Kennedy Space Center and Vandenberg AFB, California for safety prediction at missile-test ranges. The conventional Gaussian model was selected for this report. The rationale for this selection is presented in Section IV, which also includes discussion of the calculation technique for determining downwind, ground-level concentrations and the hazard corridor to be evacuated.

SECTION II

DISCUSSION OF SOURCES

Discharge of the three hydrazine missile fuels, anhydrous hydrazine (N_2H_4), unsymmetrical dimethylhydrazine (UDMH) and monomethylhydrazine (MMH), into the environment can occur at Air Force fuel storage and transfer facilities, TITAN II strategic missile sites or the TITAN III space launch vehicle operational areas at the Eastern and Western Test Ranges. In addition, hydrazine and monomethylhydrazine spills are a potential problem with future space transportation systems, aircraft auxiliary power systems and starter cartridges that utilize hydrazine propellants. About 2.4 million kilograms (5.2 million pounds) of propellants are moved over 320,000 km (200,000 miles) annually (Reference 2). In addition, large quantities are stored at facilities such as Rocky Mountain Arsenal, Edwards AFB and Aerojet General Corp, CA. Small quantities are also stored at user bases all over the country. Shipments are made in trailers, railcars and drums. The quantities of chemicals and the various shipping containers are listed in Table 1 (Reference 2).

It is estimated that 0.6 million kg of N_2H_4, 0.23 million kg of MMH and 0.64 million kg of UDMH are moved annually within the United States (Reference 2). The potential for a spill during movement of propellant from the manufacturer to the storage facility and finally to the user therefore exists.

TABLE 1. PROPELLANT SHIPPING CONTAINERS AND QUANTITIES*

Liters

Propellant	Trailer	Rail Car	Drum
N_2H_4	18000	22,000	200
MMH	21000	36,000	190
UDMH	21000	36,000	180

*Reference 2

SECTION III

PROPELLANT EVAPORATION

1. Computational Procedure

To utilize atmospheric dispersion and chemical rate equations for the calculation of pollutant concentrations in the air, the amount of pollutant released into the atmosphere per unit time must first be quantified. The evaporation rate of a propellant accidentally spilled is a function of ambient air temperature, wind speed, solar radiation, dimensions of the propellant spill and its volatility and diffusion characteristics (Reference 3). In this analysis, three assumptions are made concerning the evaporation rate:

a. The spill process is adiabatic and chemically stable.

b. The propellant is spilled as a liquid without atomization.

c. Evaporation occurs at a steady-state pool temperature.

The evaporation rate was computed by the method of Mackay (Reference 3) and is a function of concentration driving force, as determined from vapor pressure; mass transfer rate, as determined by wind generated turbulence; and diffusive properties of the air-liquid interface. The methodology assumes evaporation of a pure liquid and ideal gas behavior of the film.

The rate of evaporation of a liquid pool can be described by the following equation:

$$Q_M = k_m (P_V)(MW) A_p / RT_P \qquad (1)$$

where

Q_M = mass transfer rate of propellant into the air, kg/hour.

k_m = mass transfer coefficient, m/hr.

P_V = vapor pressure of propellant, kPa.

T_P = equilibrium pool temperature, ^oK.

R = universal gas constant, 8.314 $kPa \cdot m^3/kg \cdot mole \cdot {}^oK$.

MW = molecular weight of propellants

A_p = Area of spill, m^2.

The mass transfer coefficient (k_m) is a function of the mean wind speed ($\bar{U}$), a constant (n) related to ground roughness and the temperature profile of the atmosphere, and finally the Schmidt number defined in Appendix C (Reference 3). Although wind speed can be easily measured and the roughness factor assumed for average atmospheric conditions, the Schmidt number must be specifically computed for the propellant-air system at the equilibrium pool temperature.

The pool temperature (T_p) is determined from the steady state energy balance equation:

$$Q_G + Q_H + Q_S + Q_A = Q_E + H_E \qquad (2)$$

where

Q_G = the convective heat transfer from the ground and pool, J/hr

Q_H = the convective heat transfer from the atmosphere, J/hr

Q_S = solar insolation, J/hr

Q_A = radiative heat transfer from the atmosphere, J/hr

Q_E = radiative heat emission from the pool of liquid, J/hr

H_E = heat loss from the pool due to evaporative cooling, J/hr

The basic assumption regarding evaporation is that the liquid pool temperature is in a quasi steady-state. The calculated pool temperature is defined as that equilibrium temperature which results in a zero energy exchange between the pool and the environment. The pool temperature that satisfies the energy balance must be computed by trial and error.

As a starting point for the computations, the liquid pool temperature is assumed equal to the air temperature. Based upon this assumption, the air-propellant vapor film, the liquid propellant properties and the mass transfer rate coefficient are calculated. The Newton-Raphson iterative method is used to calculate the specific pool temperature which satisfies the energy balance. Iterative computations continue until the change in successive pool temperatures is less than 0.001°C. The pool temperature will rarely be equal to the air temperature due to radiative heat transfer and evaporative cooling. Mackay states that "Clearly, it is inaccurate to assume that the pool temperature will equal the air temperature" (Reference 3).

The pool temperature computed by the Newton-Raphson method is then compared to the originally assumed pool temperature upon which the vapor and liquid pool properties and mass transfer rate coefficient were cal-

culated. If the difference is greater than 0.1°C a fractionally modified temperature is calculated in a second iteration set and new vapor and liquid propellant properties and a new new mass transfer rate coefficient are calculated. These are then used for another solution to the equilibrium pool temperature. The procedure is continued until successive values differ by less than 0.1°C (See the computer flow chart in Appendix B). A detailed description of the pool temperature and evaporation rate equations is presented in Appendix A.

2. Evaporation Rates

Figures 1 through 3 illustrate N_2H_4, MMH and UDMH evaporation rates for typical trailer, railcar or drum transportation conditions. Dashed lines specify rates used to illustrate sample dispersion problems in Section IV. Evaporation rates were calculated for three ambient air temperatures using the computer program described in Appendices A and B with the following assumptions;

a. The ground temperature is equal to the ambient air temperature.

b. Wind speed is assumed constant.

c. The daily maximum solar insolation (R_s) rates used are $2.5(10^6)$ J/m^2·hr for a 0°C clear winter day, $3.1(10^6)$ J/m^2·hr for a 15°C clear spring day, $3.8(10^6)$ J/m^2.hr for a 30°C clear summer day.

d. The depth of spill is assumed constant at 2.5 cm.

3. Sensitivity Analysis of Evaporation Input Data

Nine input parameters were selectively varied to assess their effects on the propellant evaporation rate. Table 2 summarizes the parameters and presents a qualitative evaluation of their effect on the propellant evaporation rate. The model is most sensitive to spill area, ground temperature, ground roughness and propellant type. Solar insolation, wind speed and air temperature represent medium sensitive parameters as does ground temperature when it is below the pool temperature and heat transfer by conduction occurs. When solar insolation is below 0.8 MJ/m^2·hr, typical of times one to two hours after sunrise and one to two hours before sunset, evaporation is insensitive to insolation. Variations in pool depth and atmospheric emissivity cause no significant change in the evaporation rate.

Sensitivy analyses indicate that an error in spill area results in a proportional error in the evaporation rate. Since irregular spill areas may be difficult to measure, assessment of this parameter may result in the largest error to the evaporation rate. A 10°C error in the ground temperature (T_G) results in a 24 percent error in the evaporation rate when T_G is below the pool temperature. When T_G exceeds the pool temperature, 10°C error in $T_G$results in a 55 percent error in the evaporation rate. A variation of the roughness factor (n is assumed 0.25 for turbulent atmospheric conditions, $\Delta T = -4.18$°C/1000 feet) between 0.1 and 0.5 results in evaporation rates between 1220 and 140 kg/hour, respectively. Observed values of n have ranged from $0.04 < n < 0.93$.

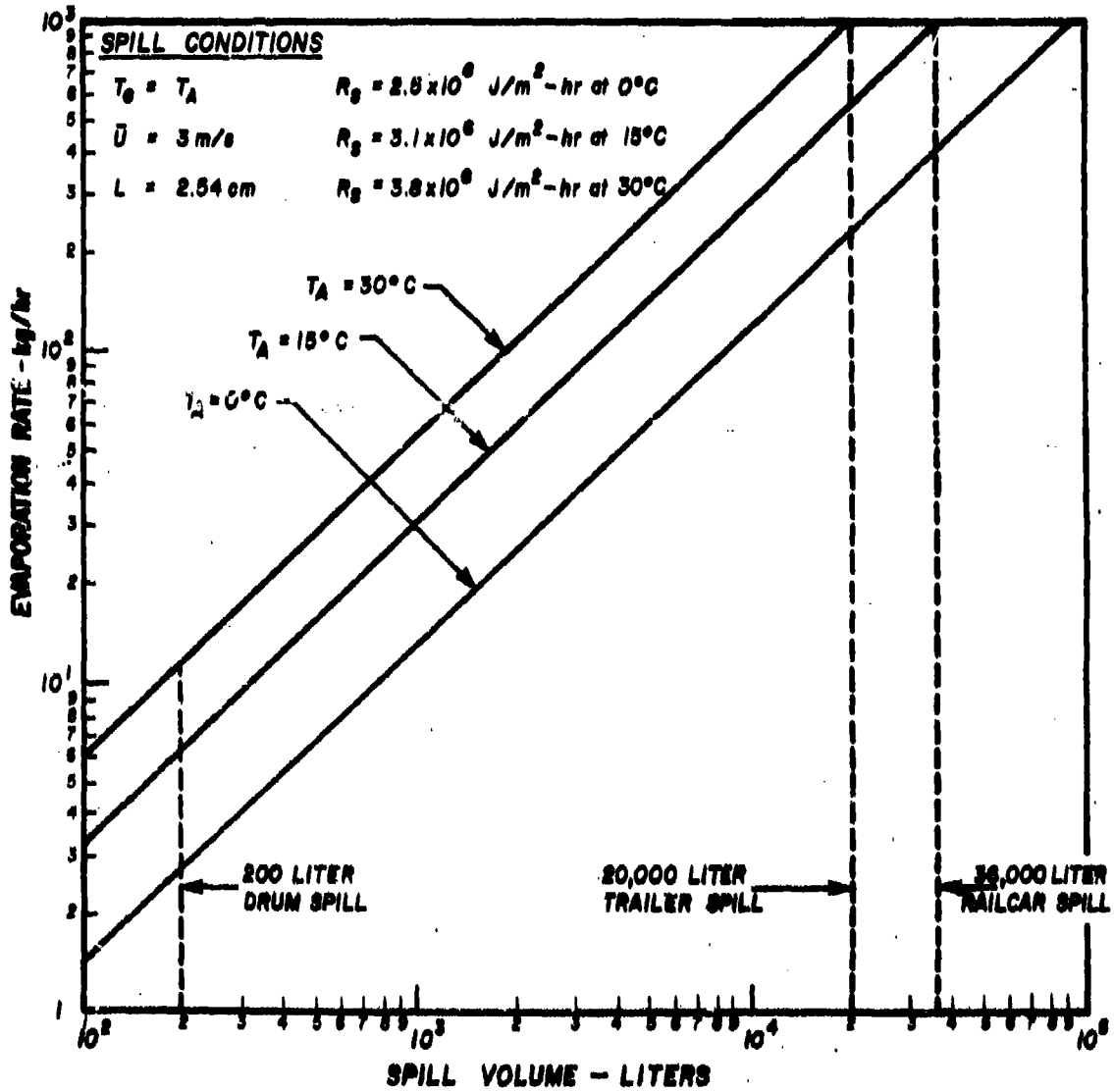

Figure 1. Hydrazine Propellant Evaporation Rates as a Function of Ambient Air Temperature and Spill Volume.

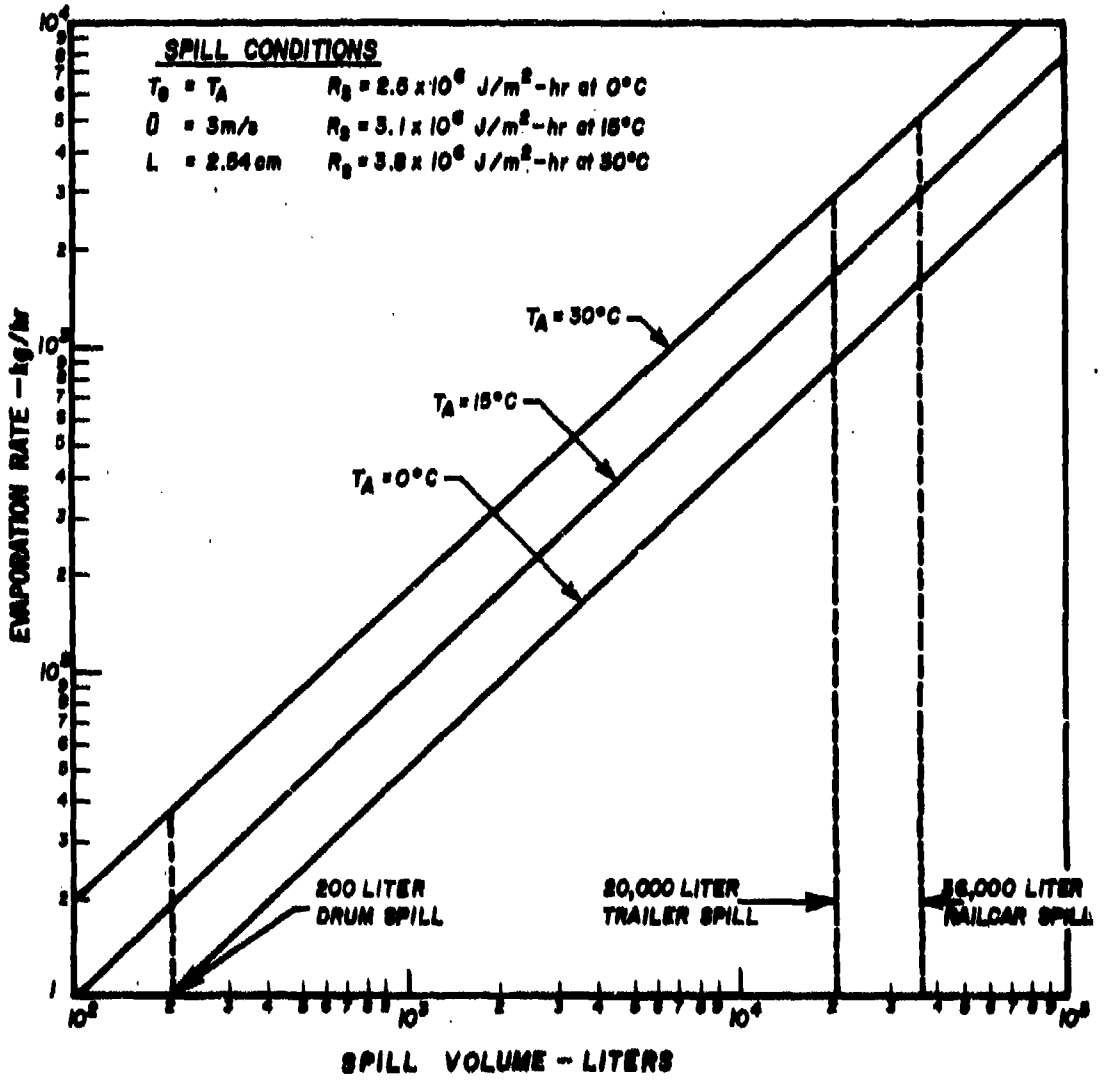

Figure 2. MMH Propellant Evaporation Rates as a Function of Ambient Air Temperature and Spill Volume.

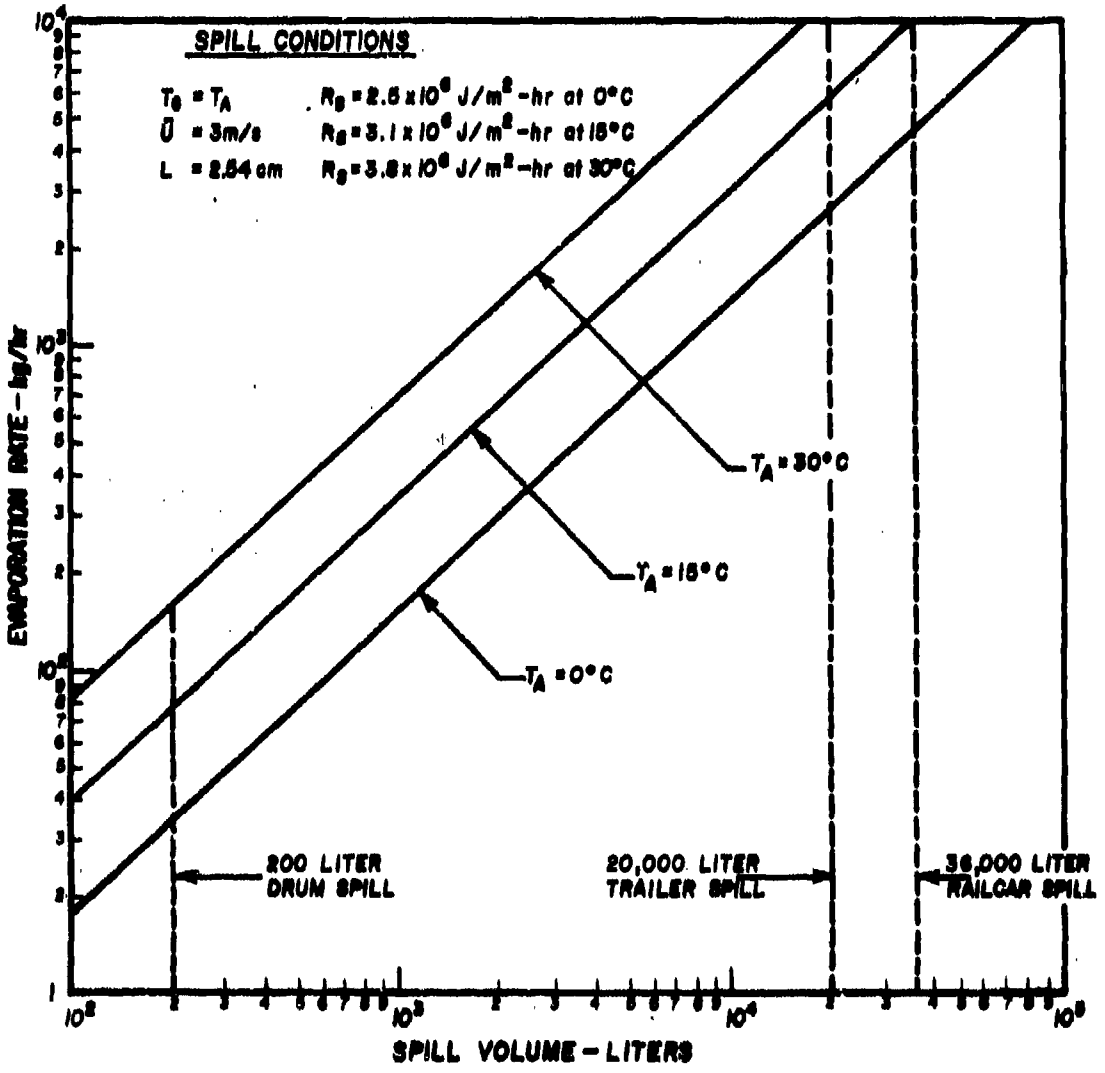

Figure 3. UDMH Propellant Evaporation Rates as a Function of Ambient Air Temperature and Spill Volume.

Analyses indicate that evaporation rates can be an order of magnitude different from those obtained using the same evaporation model without heat gain and losses to the evaporating pool. For example, a hydrazine spill covering an area of 745 m^2 evaporates at 615 kg/hr, rather than 170 kg/hr, when heat load input data are considered. This example was calculated for a windspeed of 2.6 m/s, $T_G = T_A = 17.8^{\circ}C$ and $R_s = 3.8$ $MJ/m^2 \cdot hr$. In general, one may state that the evaporation rates of UDMH and MMH, for similar meteorological and spill conditions, are eleven and three times that of hydrazine, respectively. The detailed sensitivity analysis is presented in Appendix C.

Comparison of predicted and observed evaporation rates show good agreement for initial (first hour average) evaporation rates. Experiments were conducted in fume exhaust hoods under controlled air flows and room temperatures and outdoors, during both cloudy and sunny days. Results indicate that the model fails to predict an observed decrease in evaporation rate with time. The discrepancy appears to be due to the absorption of andreaction with atmospheric carbon dioxide and water vapor (Reference 4)

TABLE 2. QUALITATIVE SENSITIVITY EVALUATION OF EVAPORATION RATE TO INPUT VARIABLES

Input Variables		Sensitivity		
Symbol	Name	High	Medium	Low
KP*	Propellant Type	+		
T_G	Ground Temperature	+	+	
A_p	Area of Spill	+		
R_s	Solar Insolation		+	+
$\bar{U}$	Wind speed		+	
L	Spill Depth			+
T_A	Air Temperature		+	
n	Ground Roughness Factor	+		
ϵ_a	Emissivity of the Atmosphere			+

*KP = 1, 2, 3 • 1 - N_2H_4, 2 - MMH, 3 - UDMH

SECTION IV

ATMOSPHERIC DISPERSION MODEL

1. Computational Procedure

A simple, point source Gaussian plume model was selected to describe the dispersion of propellant vapors released into the atmosphere. A comparison of Gaussian models, Non-Gaussian models, including the temperature-difference model used for safety prediction at AF missile sites, box models and the gradient transport models have shown the Gaussian calculation technique to be the method of choice for generalized usage. Experimental diffusion studies by Cramer, Haugen, Pasquill and others have confirmed the virtues of the Gaussian distribution function and have concluded that "the Gaussian plume formula should have a wide area of practical applicability in the atmosphere" (Reference 5).

The Environmental Protection Agency (EPA) has concluded that "Gaussian models are generally state-of-the-art techniques for estimating the impact of non-reactive pollutants; (Reference 6). Furthermore, Gaussian models represent the best choice for most point source evaluations and have been found to provide reasonable concentration estimates (accuracy by a factor of 2) in flat or gently rolling terrain (Reference 6). Although Gaussian models have been praised in terms of simplicity, flexibility and good correlations between predicted and measured downwind concentration values, they are subject to the following assumptions and limitations:

a. The terrain in the region of interest is either flat or gently rolling.

b. No topographic obstructions occur in the vicinity of the source.

c. The wind speed direction and other meteorological conditions remain uniform and constant with height.

d. Aerodynamic downwash does not occur.

The following equation is used to calculate ground level concentrations for a point source, continuous release emission into the atmosphere:

$$C_{(xy)} = \frac{10^6 \ Q_M}{3600 \ \pi \ \sigma_y \ \sigma_z \ \bar{U}} \exp - \left[\frac{1}{2}\left(\frac{Y}{\sigma_y}\right)^2\right] \qquad (3)$$

where

$C_{(xy)}$	= concentration at coordinates x, y, mg/m^3
Q_M	= mass transfer rate of propellant into the air, kg/hr
$\bar{U}$	= average surface wind speed, m/sec
σ_y, σ_z	= standard deviation of the concentration distribution along the y (crosswind) and z (vertical axes).
x, y, z	= orthogonal coordinate system in which the origin is at ground level and x is in the downwind direction.
3600	conversion factor for time

This equation is applicable for ground level sources, such as a spill, with no effective plume rise.

The constants used to calculate the sigma y and sigma z coefficients are illustrated in Tables 3 and 4 for various stability categories and downwind distances. These coefficients are currently used in various EPA models (Reference 6) and are consistent with Turner's Workbook. (Reference 6).

Equation 3 is applicable during conditions when the plume is unrestricted in its vertical expansion. During inversions, the vertical expansion of the plume is restricted when it reaches the lower base of a stable air mass. This type of inversion occurs most frequently during the late night and early morning hours. The vertical concentration profile becomes uniform and is represented by the following equation (Reference 7):

$$C_{(xc)} = \frac{10^6 Q_M}{3600\sqrt{2\pi}\,\sigma_y H_M \bar{U}} \exp\left[\frac{1}{2}\left(\frac{Y}{\sigma_y}\right)^2\right] \qquad (4)$$

where H_M = height from ground level to the base of the stable layer in meters

A reasonable assumption is that the vertical concentration profile begins to be affected by the lid at that distance (X_L) downwind from the source where concentration at the stable layer boundary is one tenth of the plume centerline concentration. X_L is that downwind distance from the source where σ_z equals $H_M/2.15$. It can be easily determined by using Figure 4 and noting the downwind distance where σ_z equals $H_M/2.15$ (Reference 7). At $2X_L$ and greater one can assume the vertical concentration gradient to be uniform and equation 4 to be applicable.

TABLE 3. CONSTANTS USED TO CALCULATE σ_y IN EPA DEVELOPED DISPERSION PROGRAMS (REFERENCE 6)

$$\sigma_y = \frac{1000 \times \sin \theta}{2.15 \quad \cos \theta} = 465.12 \times \tan \theta$$

x = downwind distance in kilometers

Stability (Categories*)	Value of θ (degrees)
A	$24.167-2.5334 \log_e x$
B	$18.333-1.8096 \log_e x$
C	$12.5-1.0857 \log_e x$
D	$8.333-.72382 \log_e x$
E	$6.25-.54287 \log_e x$
F	$4.1667-.36191 \log_e x$

*Stability Categories are based on data in Turner's Workbook of Atmospheric Dispersion Estimates (Reference 7).

TABLE 4. CONSTANTS USED TO CALCULATE σ_z IN EPA DEVELOPED PROGRAMS

(REFERENCE 6)

$$\sigma_z = ax^b$$

Stability (Categories*)	Downwind Distance (x) (kilometer)	Values for σ_z (m) a	b
A	<0.1	122.8	0.9447
	0.1 - 0.15	158.0	1.0542
	0.15 - 0.2	170.22	1.0932
	0.2 - 0.25	179.52	1.1262
	0.25 - 0.3	217.41	1.2644
	0.3 - 0.4	258.89	1.4094
	0.4 - 0.5	346.75	1.7283
	0.5 - 3.11	453.85	2.1166
	>3.11	**	
B	<0.2	90.673	0.93198
	0.2 - 0.4	98.483	0.98332
	0.4 - 35.0	109.30	1.0971
	>35	**	
C	<123.0	61.141	0.91465
	>123.0	**	
D	<0.3	34.459	0.86974
	0.3 - 1.0	32.093	0.81066
	1.0 - 3.0	32.093	0.64403
	3.0 - 10.0	33.504	0.60486
	10.0 - 30.0	36.650	0.56589
	>30.0	44.053	0.51179
E	<0.1	24.260	0.83660
	0.1 - 0.3	23.331	0.81956
	0.3 - 1.0	21.628	0.75660
	1.0 - 2.0	21.628	0.63077
	2.0 - 4.0	22.534	0.57154
	4.0 - 10.0	24.703	0.50527
	10.0 - 20.0	26.970	0.46714
	20.0 - 40.0	35.420	0.37615
	>40	47.618	0.29592

**The maximum calculated value for σ_z is 5000 meters.
*Stability Categories are based on data in Turner's Workbook of Atmospheric Dispersion Estimates (Reference 7).

TABLE 4 (Continued)

Stability (Categories*)	Downwind Distance (x) (kilometers)	Values for σ_z (m) a	b
F	<0.2	15.209	0.81558
	0.2 - 0.7	14.457	0.78407
	0.7 - 1.0	13.953	0.68465
	1.0 - 2.0	13.953	0.63227
	2.0 - 3.0	14.823	0.54503
	3.0 - 7.0	16.187	0.46490
	7.0 - 15.0	17.836	0.41507
	15.0 - 30.0	22.651	0.32681
	30.0 - 60.0	27.074	0.27436
	>60.0	34.219	0.21716

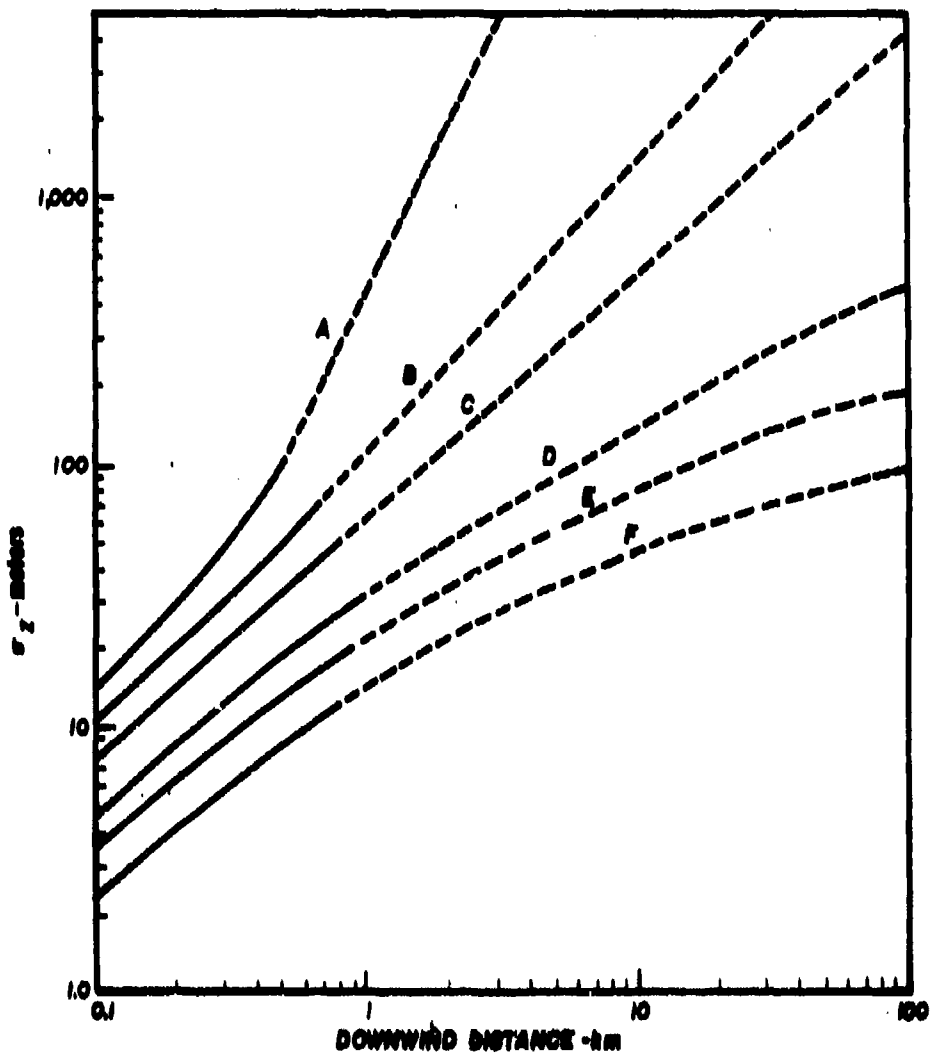

Figure 4. Vertical Dispersion Coefficient as a Function of Downwind Distance from the Source.

2. Dispersion Examples

A sample dispersion problem is presented to demonstrate the solution technique for calculating the downwind, ground level, centerline concentration and the crosswind distance to a specific concentration limit. The spill sizes and specific evaporation rates assumed were taken from Figures 1-3, for a 15°C ambient air temperature. The ground level centerline plume concentration is calculated using the following Gaussian equation:

$$C_x = \frac{10^6 \, Q_M}{3600 \, \pi \, \sigma_y \sigma_z \bar{U}} \qquad (5)$$

Equation 5 assumes a high mixing layer boundary and therefore, minimum vertical restriction of the plume. A 3m/sec windspeed and Class B stability category representing strong to moderate solar radiation, were selected for this example (Reference 7). Table 5 lists EPA calculated horizontal and vertical dispersion coefficients applicable to this problem based on the constants described in Tables 3 and 4. Table 6 lists the center-line concentrations computed for a specific spill size using Equation 5. The following formula is used to calculate the crosswind distance to a specific concentration isopleth:

$$y = \left[2 \, \ln\left(\frac{C_x}{C_{xy}}\right) \right] \sigma_y^{1/2} \qquad (6)$$

where Y = crosswind distance from the plume centerline to the 5TPL

C_{xy} = crosswind concentration isopleth = 7 mg/m^3 for N_2H_4

C_x = downwind centerline concentration, mg/m^3

This equation is useful in determining the width of the hazard corridor associated with any selected limiting concentration. For hydrazine a reasonable limiting value is 7 mg/m^3, the 1 Hour Short-Term Public Limit (STPL) (Reference 8). The STPL for MMH and UDMH are 2.8 and 38.2 mg/m^3 respectively. These values are used in Figures 5-7 and 17-19. Table 7 lists the downwind distance, centerline concentration, and crosswind distance to the 7 mg/m^3 isopleth. Figures 5, 6 and 7 illustrate the STPL isopleths for hydrazine, MMH, and UDMH, based on spill conditions

TABLE 5. Calculated Standard Deviations Used in Sample Dispersion Problem*

Downwind Distance (m)	Horizontal and Vertical Standard Deviations σ_y (m)	σ_z (m)
25	5.42	2.62
50	10.2	5.18
75	14.8	7.71
100	19.3	10.6
150	27.9	15.5
200	36.2	20.2
225	40.2	22.7
250	44.3	25.2
275	48.3	27.7
300	52.2	30.1
325	56.1	32.6
350	60.0	35.1
375	63.9	37.5
400	67.7	40.0
425	71.5	42.7
450	75.3	45.5
475	79.0	48.3
500	82.8	51.1
550	90.2	56.7
600	97.5	62.4
650	104.8	68.1
700	112.0	73.9
750	119.1	79.7
800	126.2	85.6
850	133.3	91.5
900	140.3	97.4
950	147.2	103.
1000	154.1	109.
1100	167.8	121.3
1200	181.4	133.5
1300	194.8	145.8
1400	208.1	158.1
1500	221.3	170.5
1550	227.9	176.8
1600	234.4	183.0

*Coefficients calculated using equations in Tables 10 and 11, Stability Category B

TABLE 6. Downwind, Ground-Level Centerline Concentration for Sample Dispersion Problem*

Downwind Distance (m)	C_x mg/m^3
100	134
150	63
200	37
225	30
250	25
275	20
300	17
325	15
350	13
375	11
400	10
425	9
450	8
475	7
500	6

*Assumes a 36000 liter spill, evaporating at 930 kg/hr (See Figure 1.)

TABLE 7. Crosswind Distance Values To The

7 mg/m^3 Hazard Corridor*

Downwind Distance (m)	Downwind, Ground-Level, Centerline Concentration (mg/m^3)	Crosswind Distance y (m)
100	134	47
150	63	58
200	37	66
225	30	69
250	25	71
275	20	70
300	17	69.5
325	15	69
350	13	67
375	11	61
400	10	57
425	9	51
450	8	39
475	7	0

*Hazard Corridor defined by the Short-Term Public Limit for Hydrazine (Reference 7). A 3600 liter spill, evaporating at 930 kg/hr is assumed. Wind Speed = 3 m/s, Stability B and unrestricted mixing depths.

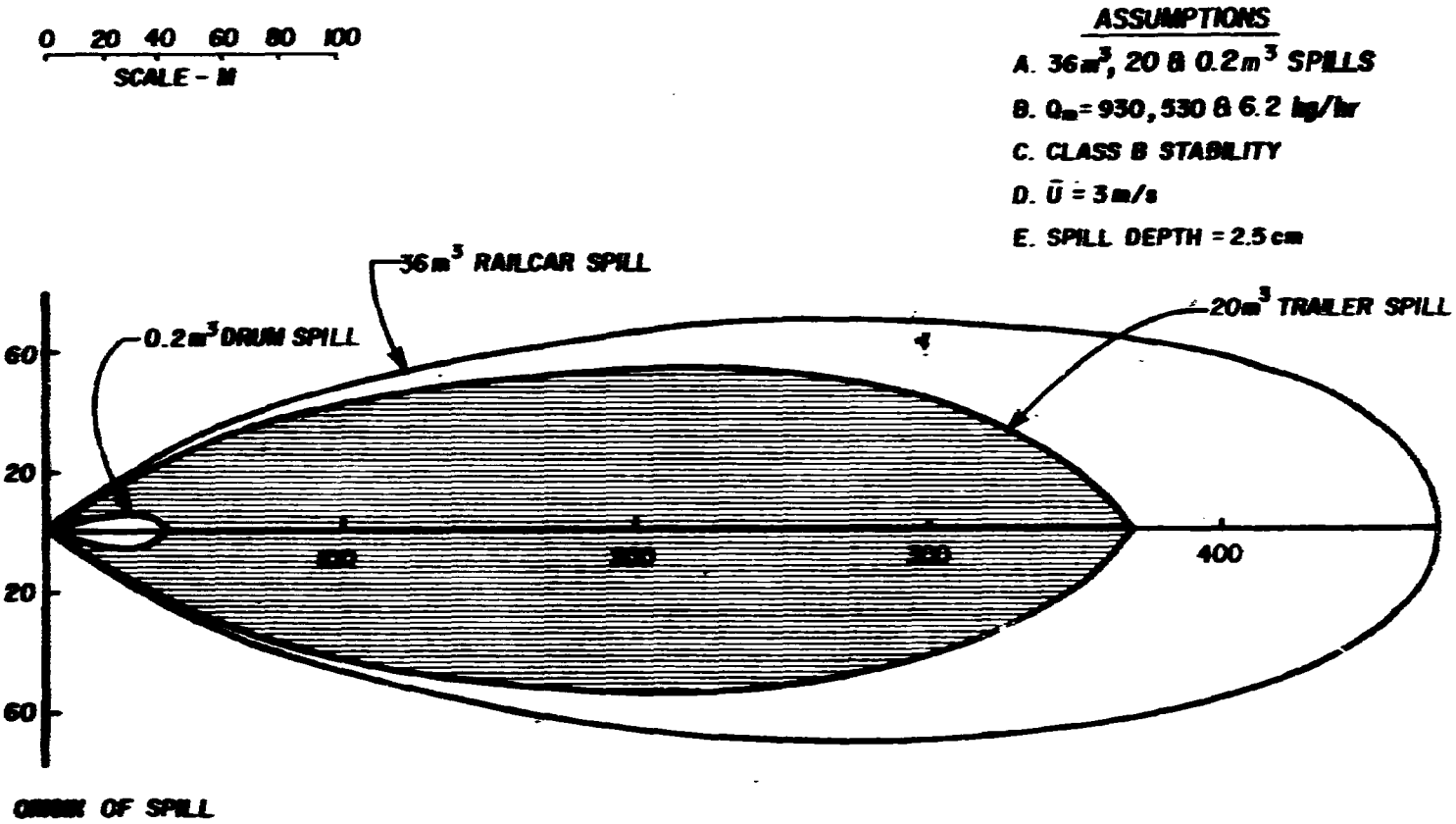

Figure 5. Illustration of the 7 mg/m^3 Short-Term Public Limit Hazard Corridor for MMH.

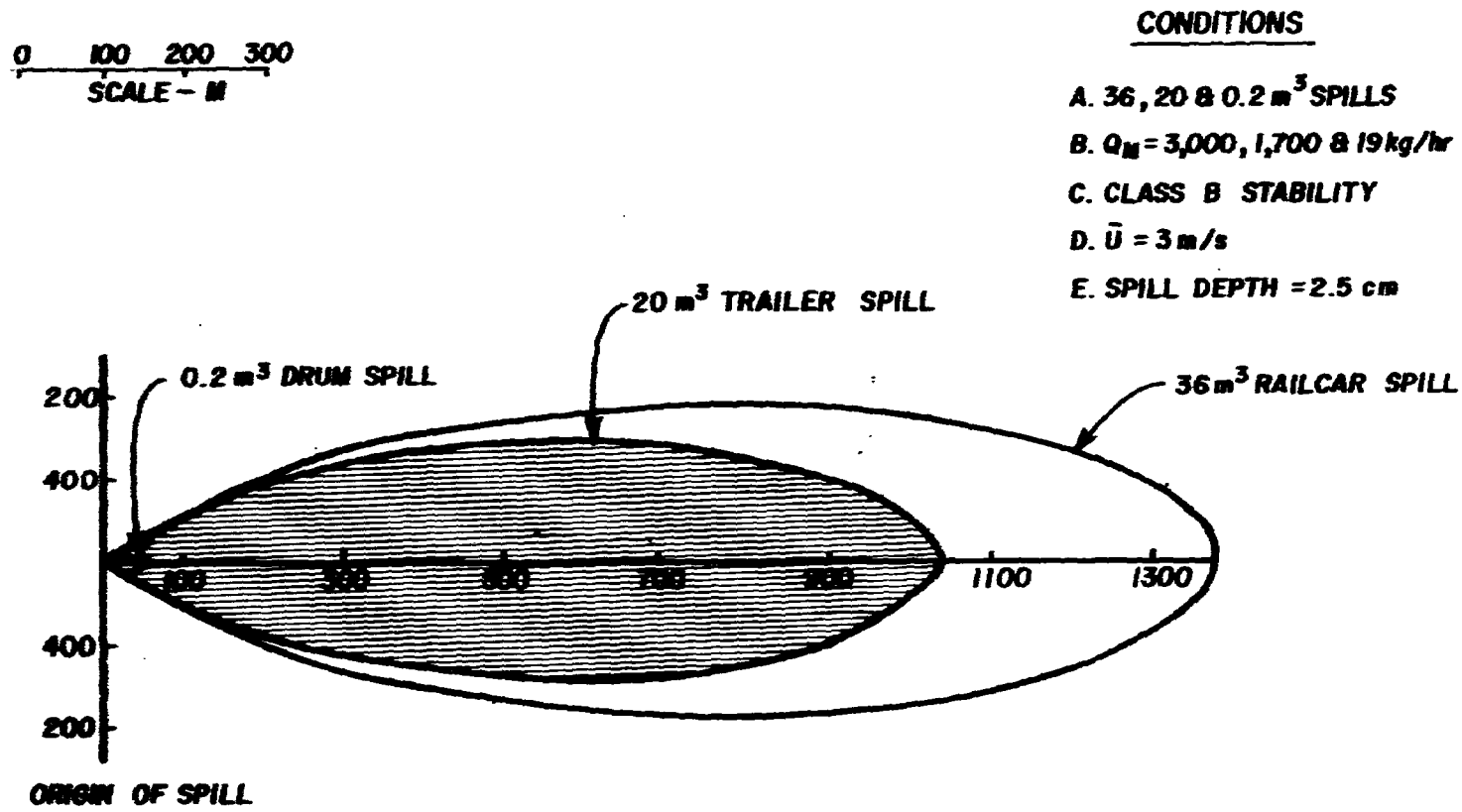

Figure 6. Illustration of the 2.8 mg/m^3 Short-Term Public Limit Hazard Cooridor for MMH.

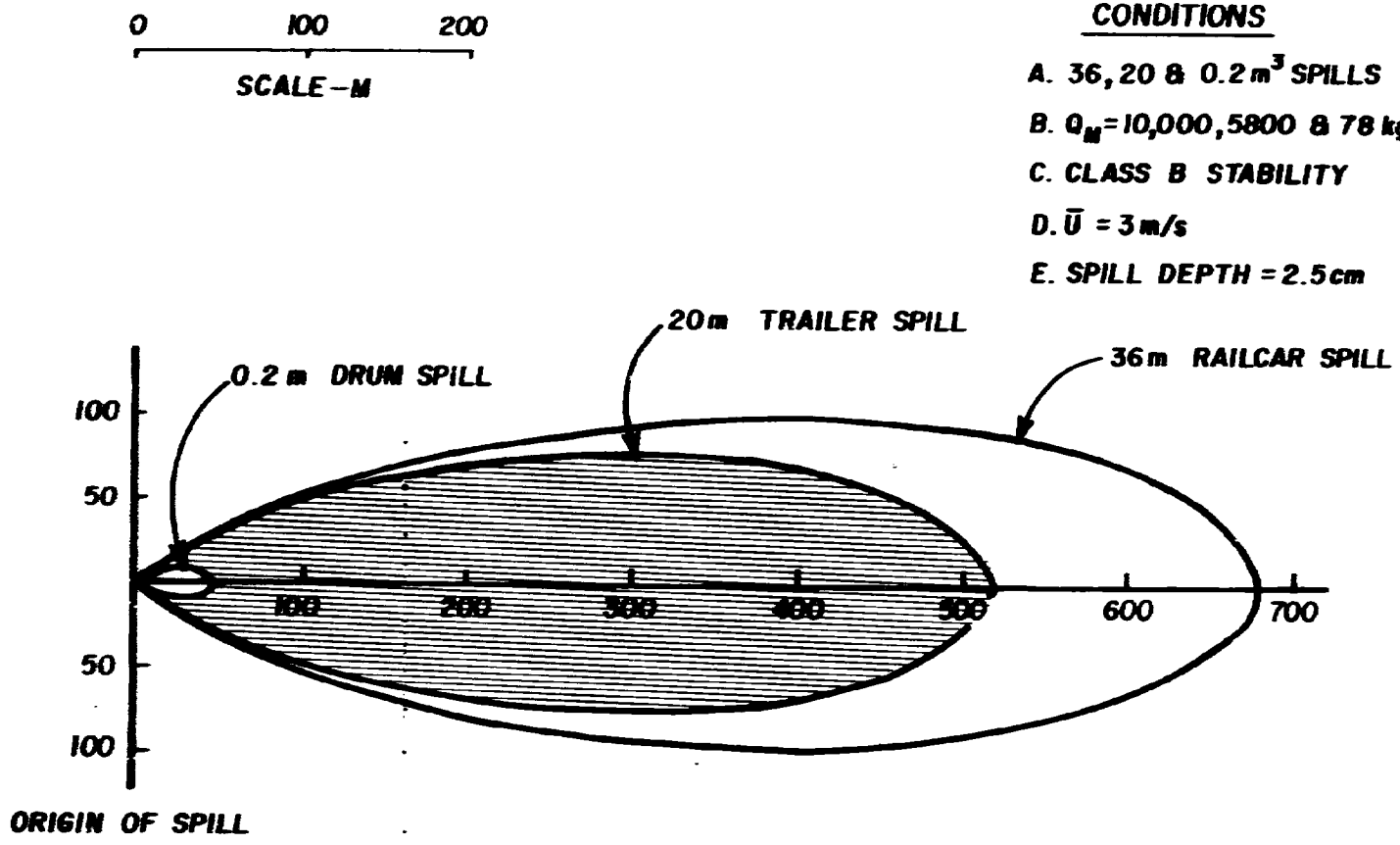

Figure 7. Illustration of the 38.2 mg/m^3 Short-Term Public Limit Hazard Corridor for UDMH.

listed in Figures 1-3, $T_A = 15^{\circ}C$, and unrestricted vertical expansion of the plume. Figures 8-16 present the hydrazine center-line ground-level concentrations for 200, 20,000 and 36,000 liter spills computed for 0, 15, and $30^{\circ}C$ ambient air temperatures. These volumes may be associated with an accidental spill for a drum, trailer or railcar, respectively. Finally, the downwind distance to the STPL, as a function of evaporation rate, for any stability category, is presented in Figures 17-19. These graphs represent a quick means for determining the downwind distance that must be evacuated to avoid exposures in excess of the STPL. These curves were calculated based on a mean wind speed of 3 m/s and on the STPL for the specific propellant. To use these curves with other wind speeds or limiting concentrations, the evaporation rate computed for a given spill situation must be modified as follows:

$$Q_2 = Q_1 \left(\frac{STPL}{C_{xy}}\right)\left(\frac{3}{\bar{U}}\right) \qquad (7)$$

where

Q_2 = evaporation rate for use in Figures 17, 18 and 19.

Q_1 = original evaporation estimate from program

C_{xy} = concentration limit, mg/m^3

$\bar{U}$ = mean wind speed, m/sec

For example, assume a hydrazine spill for the following conditions:

(a) Q_1 = 1000 kg/hr

(b) $\bar{U}$ = 6 m/sec

(c) C_{xy} = 2 mg/m^3

(d) Stability Category D

Since Figure 17 was developed for an STPL concentration of 7 mg/m^3 and a wind speed of 3m/sec; the emission estimate of 1000 kg/hr must be modified as follows:

$$Q_2 = 1000 \left(\frac{7}{2}\right)\left(\frac{3}{6}\right) \qquad (8)$$

$$Q_2 = 1750 \text{ kg/hr}$$

Q_2 can be directly applied in Figure 17 to estimate a downwind evacuation distance of 2.2 km to the 2 mg/m^3 concentration limit.

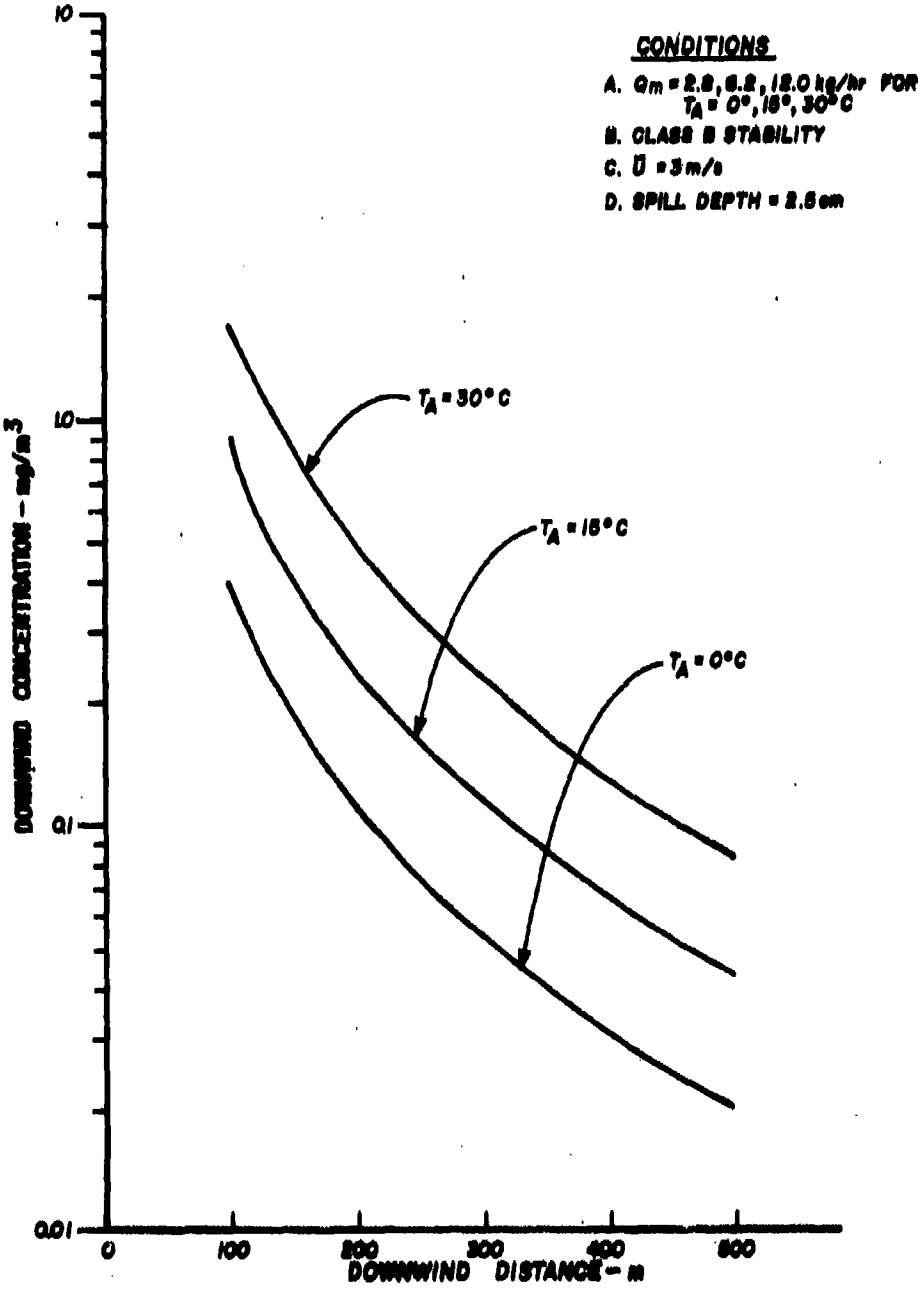

Figure 8. Downwind Ground-Level Centerline Concentrations for a 200 Liter Hydrazine Drum Spill.

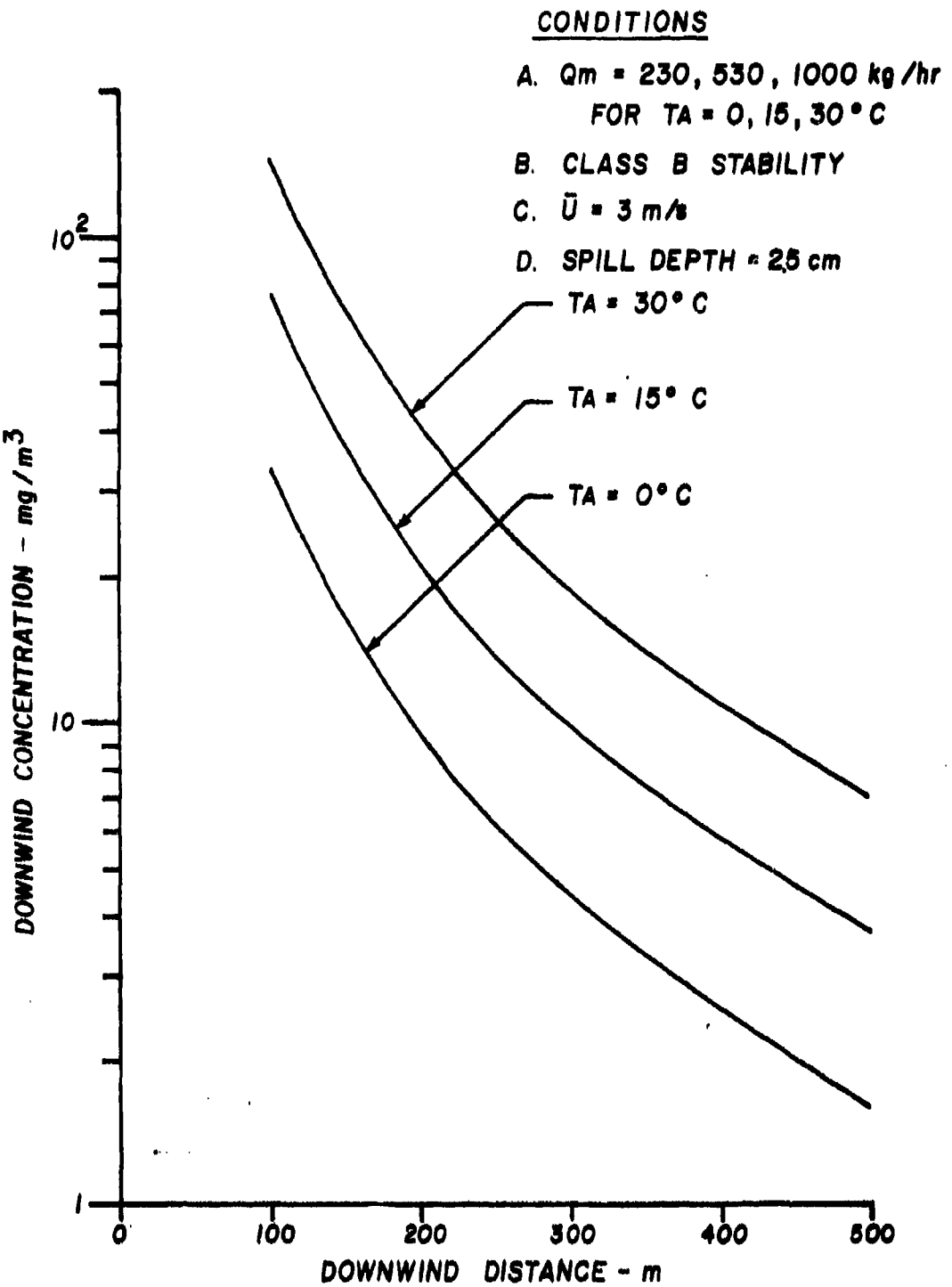

Figure 9. Downwind, Ground-Level Centerline Concentration: a 20,000 Liter Hydrazine Trailer Spill.

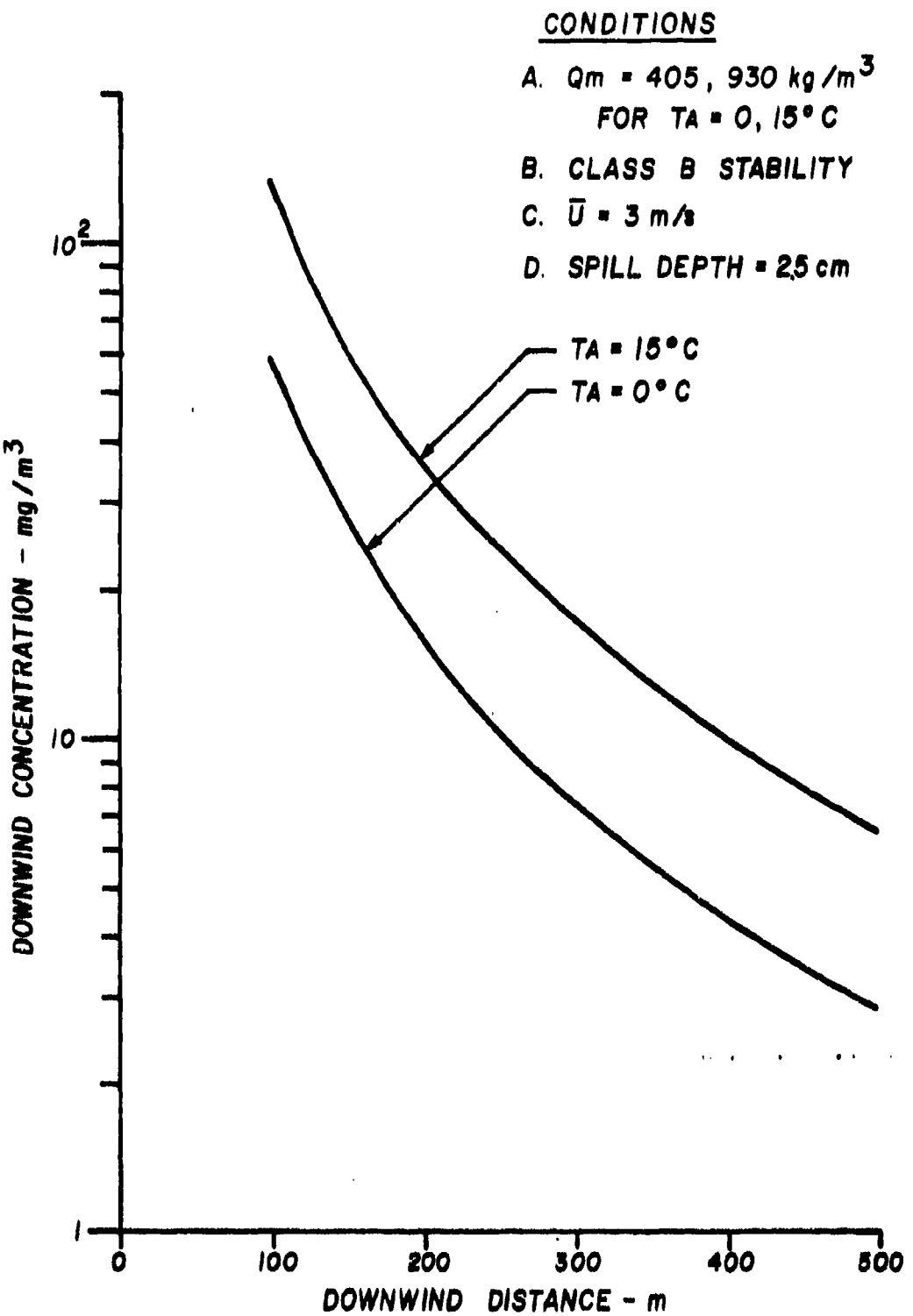

Figure 10. Downwind, Ground-Level Centerline Concentrations for a 36,000 Liter Hydrazine Railcar Spill.

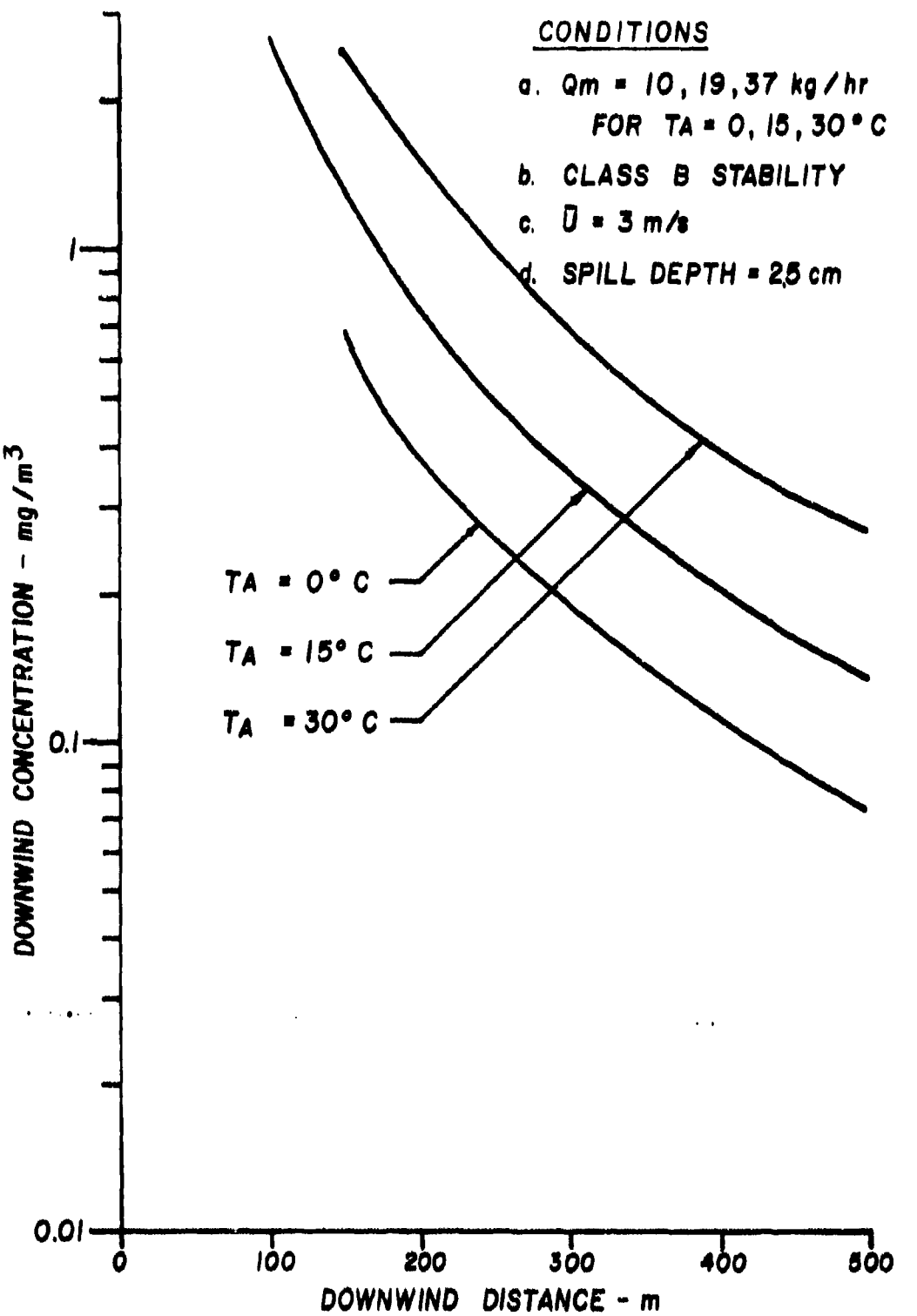

Figure 11. Downwind, Ground-Level Centerline Concentrations for a 200 Liter MMH Drum Spill.

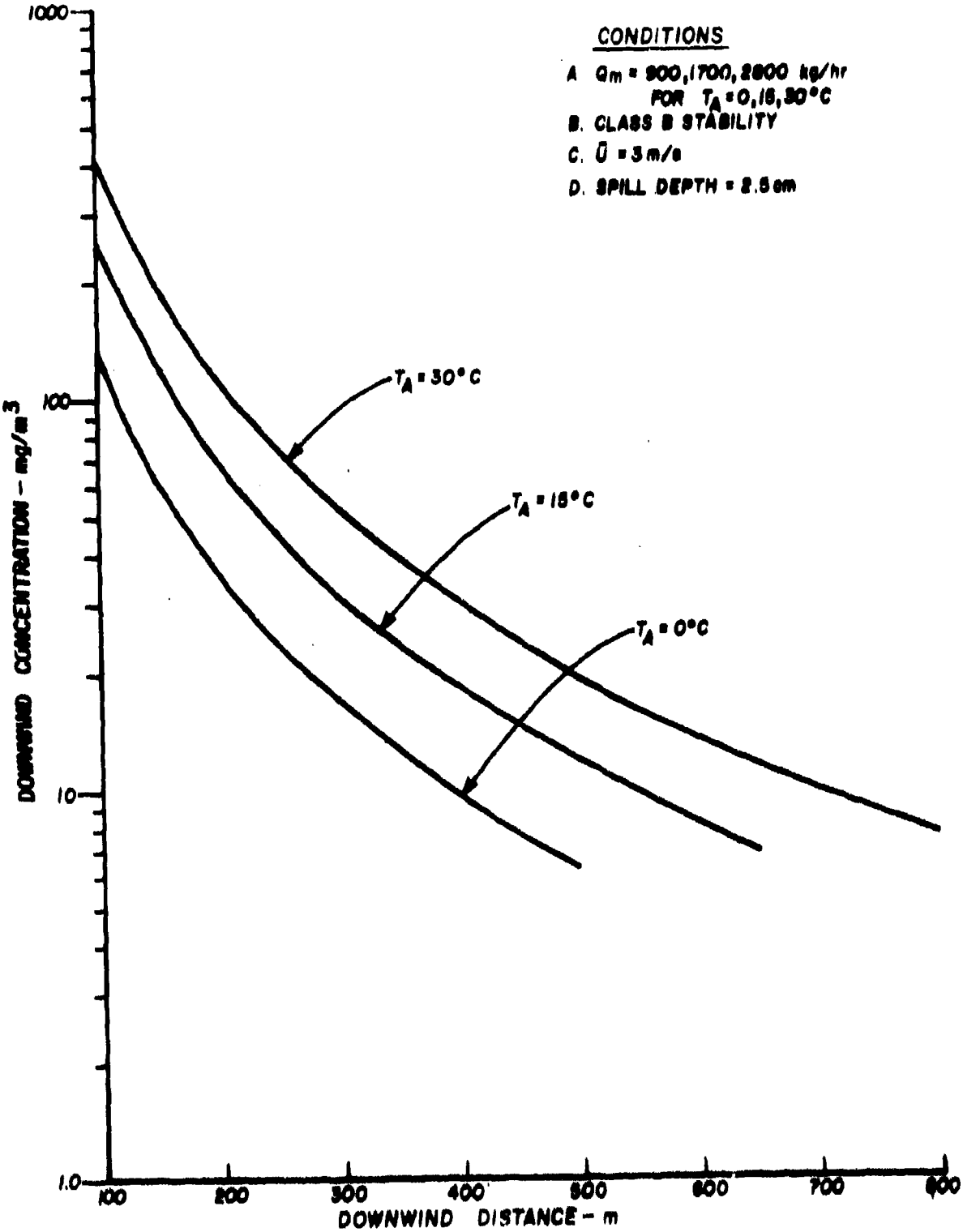

Figure 12. Downwind, Ground-Level Centerline Concentrations for a 20,000 Liter MMH Trailer Spill.

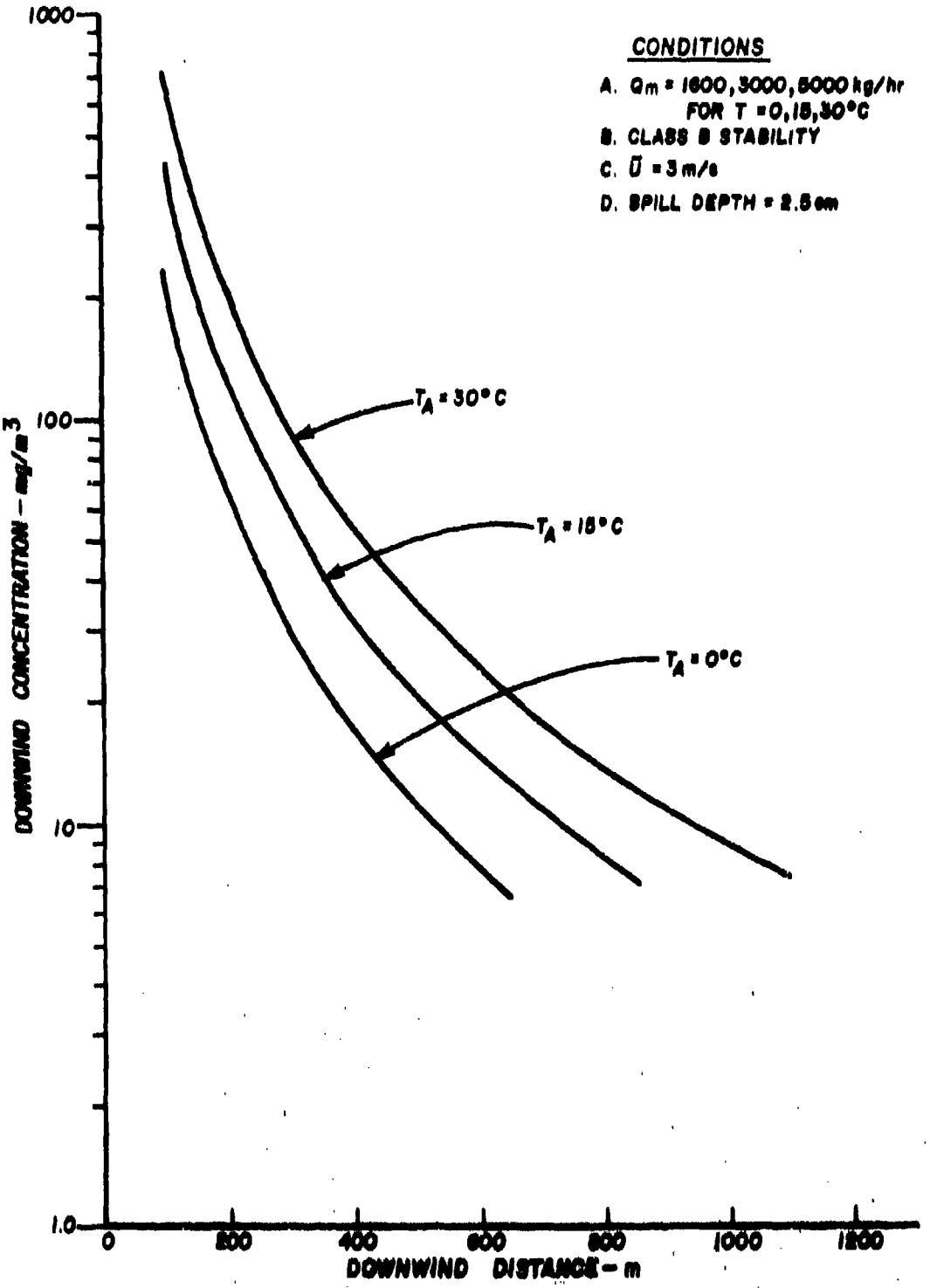

Figure 13. Downwind, Ground-Level Centerline Concentrations for a 36,000 Liter MMH Railcar Spill.

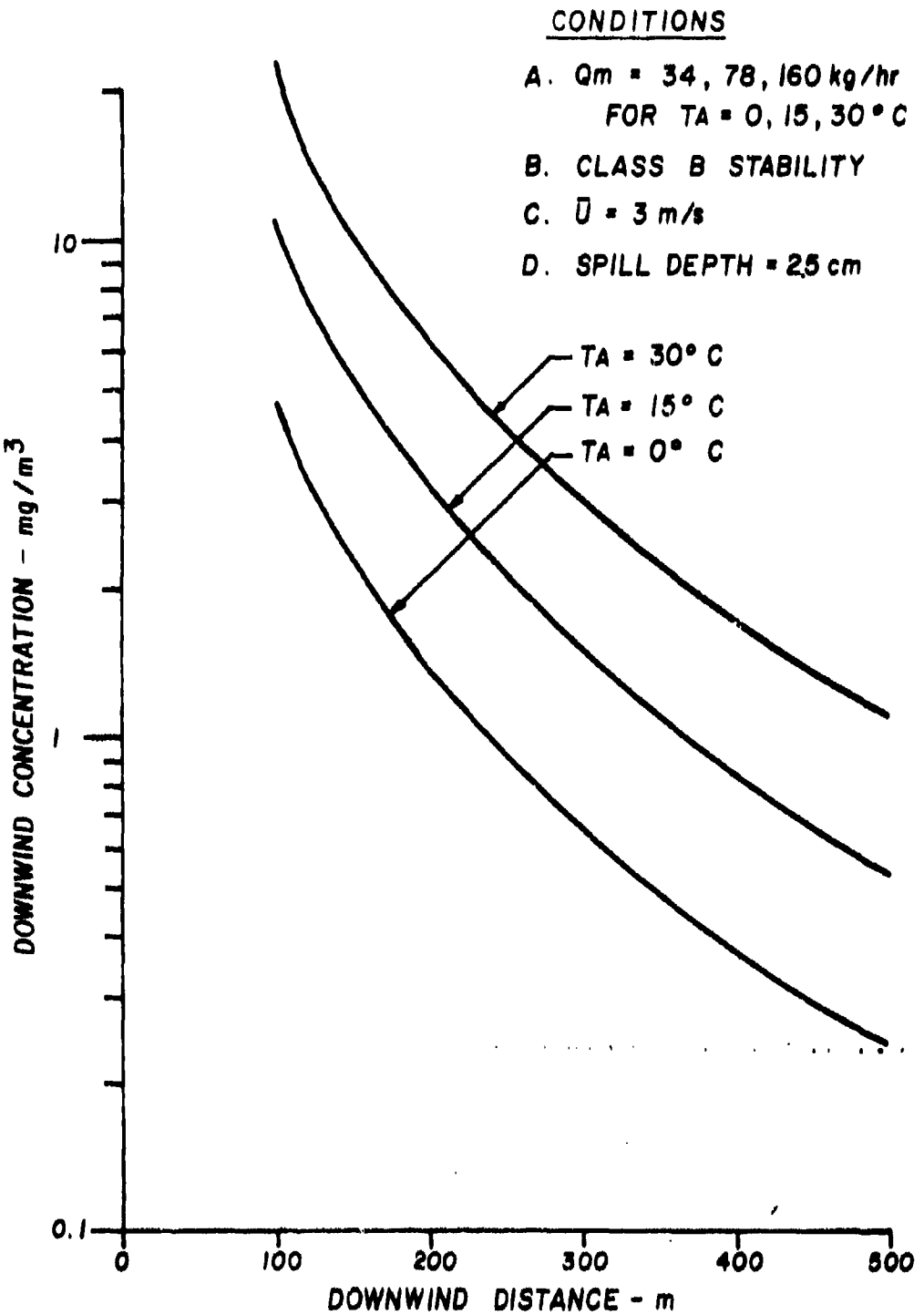

Figure 14. Downwind, Ground-Level Centerline Concentrations for a 200 Liter UDMH Drum Spill.

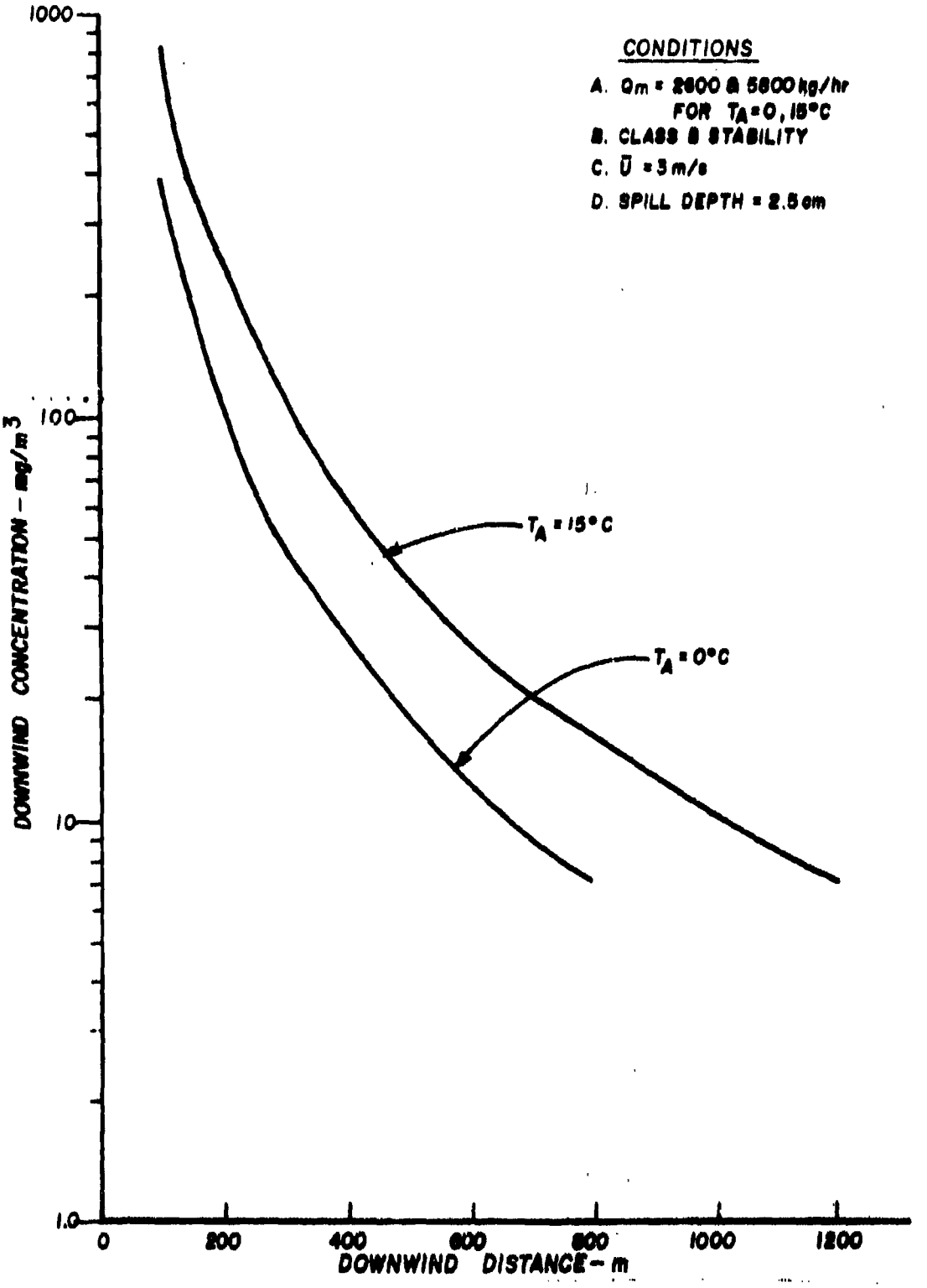

Figure 15. Downwind, Ground-Level Centerline Concentrations for a 20,000 Liter UDMH Spill.

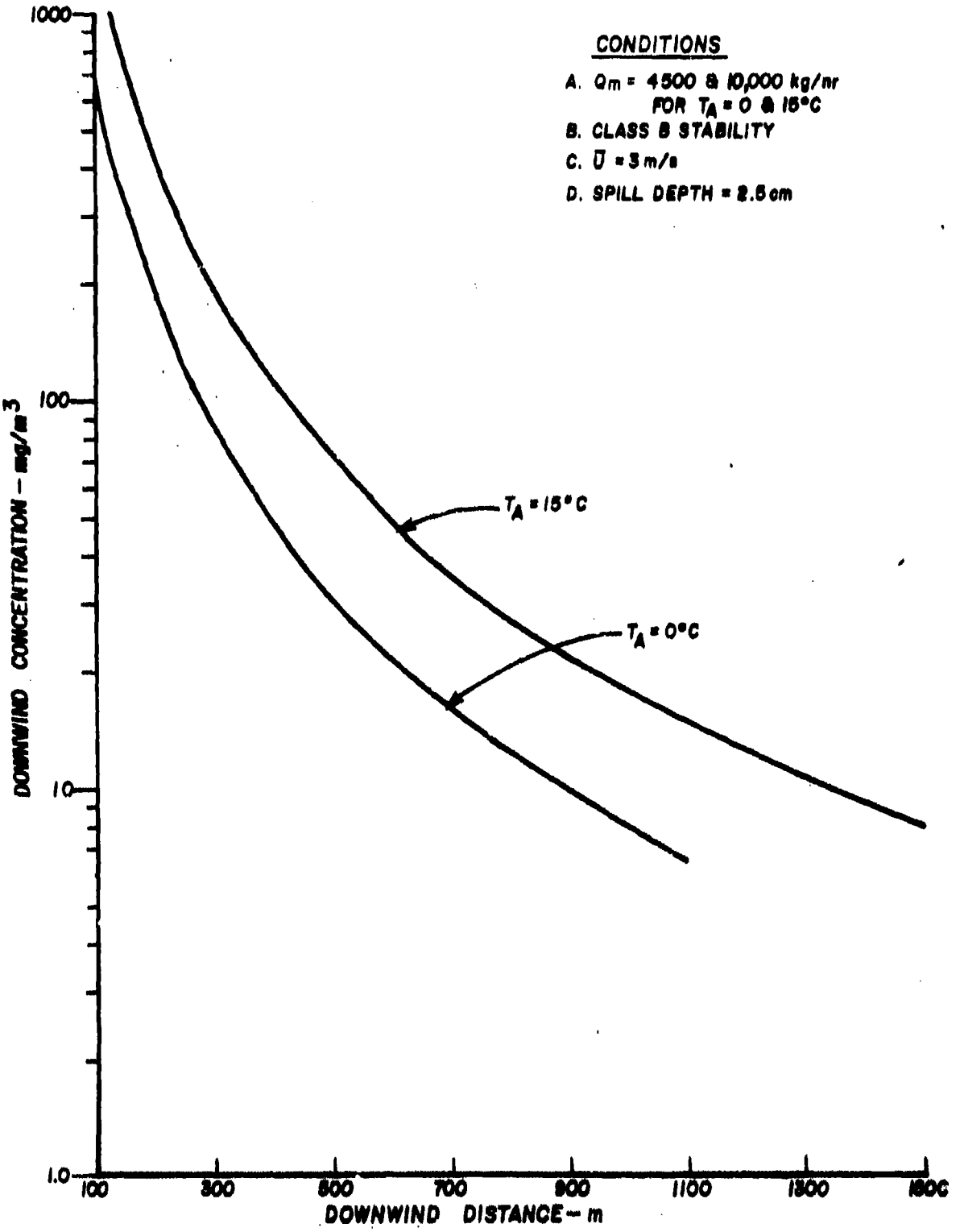

Figure 16. Downwind, Ground-Level Centerline Concentrations for a 36,000 Liter UDMH Spill.

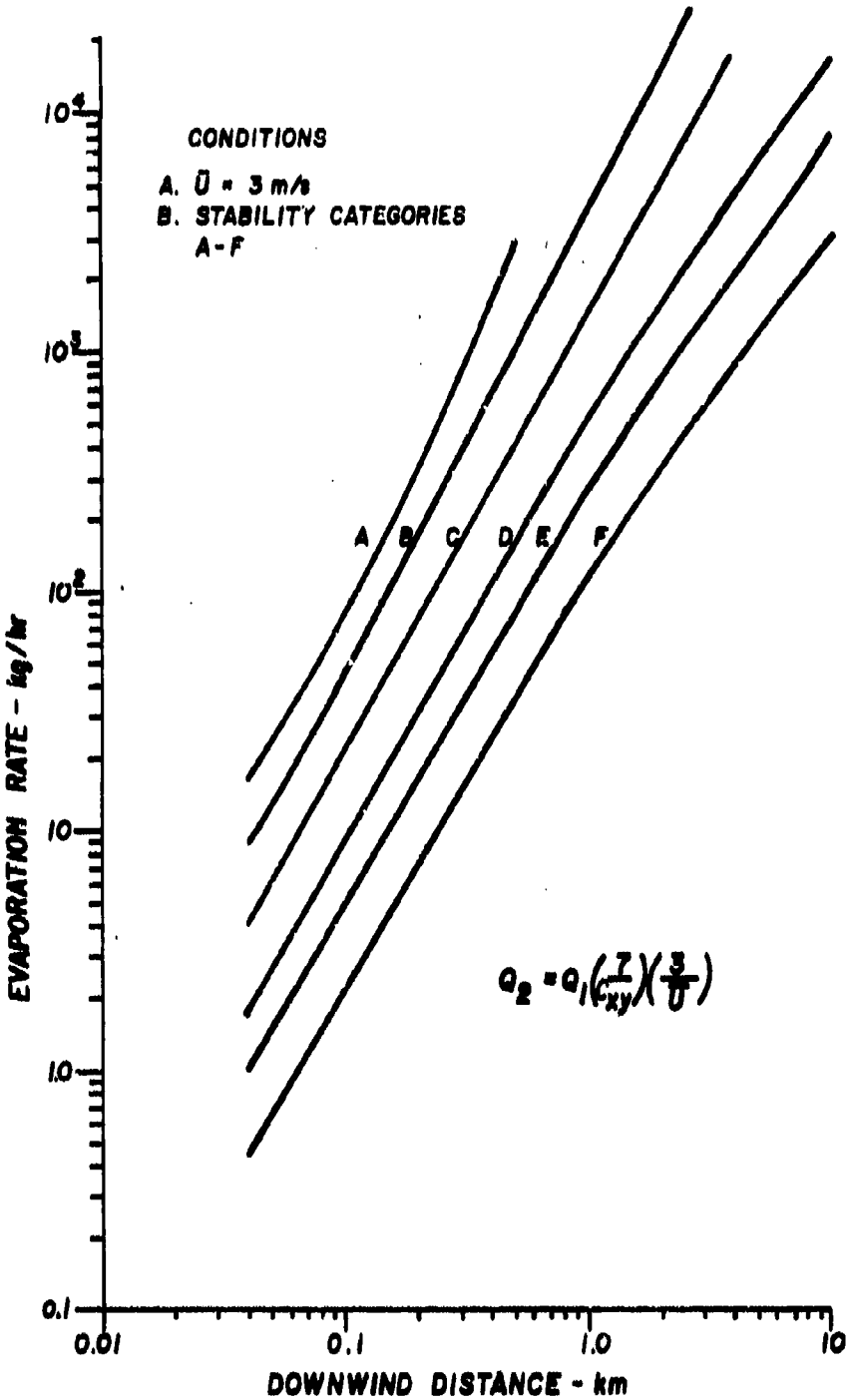

Figure 17. Downwind Evacuation Distance to the Short-Term Public Exposure Limit Concentration for Hydrazine.

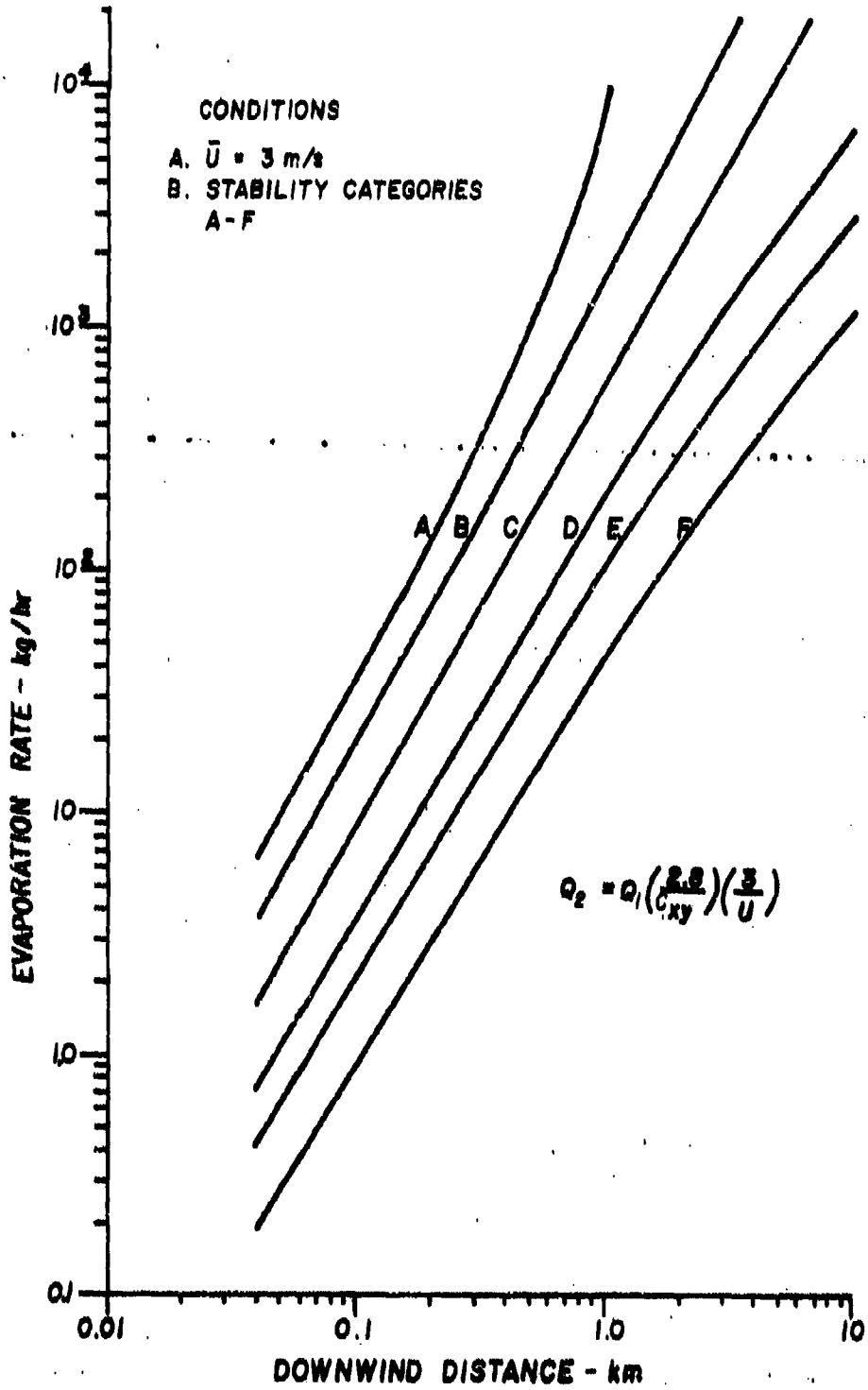

Figure 18. Downwind Evacuation Distance to the Short-Term Public Exposure Limit Concentration for MMH.

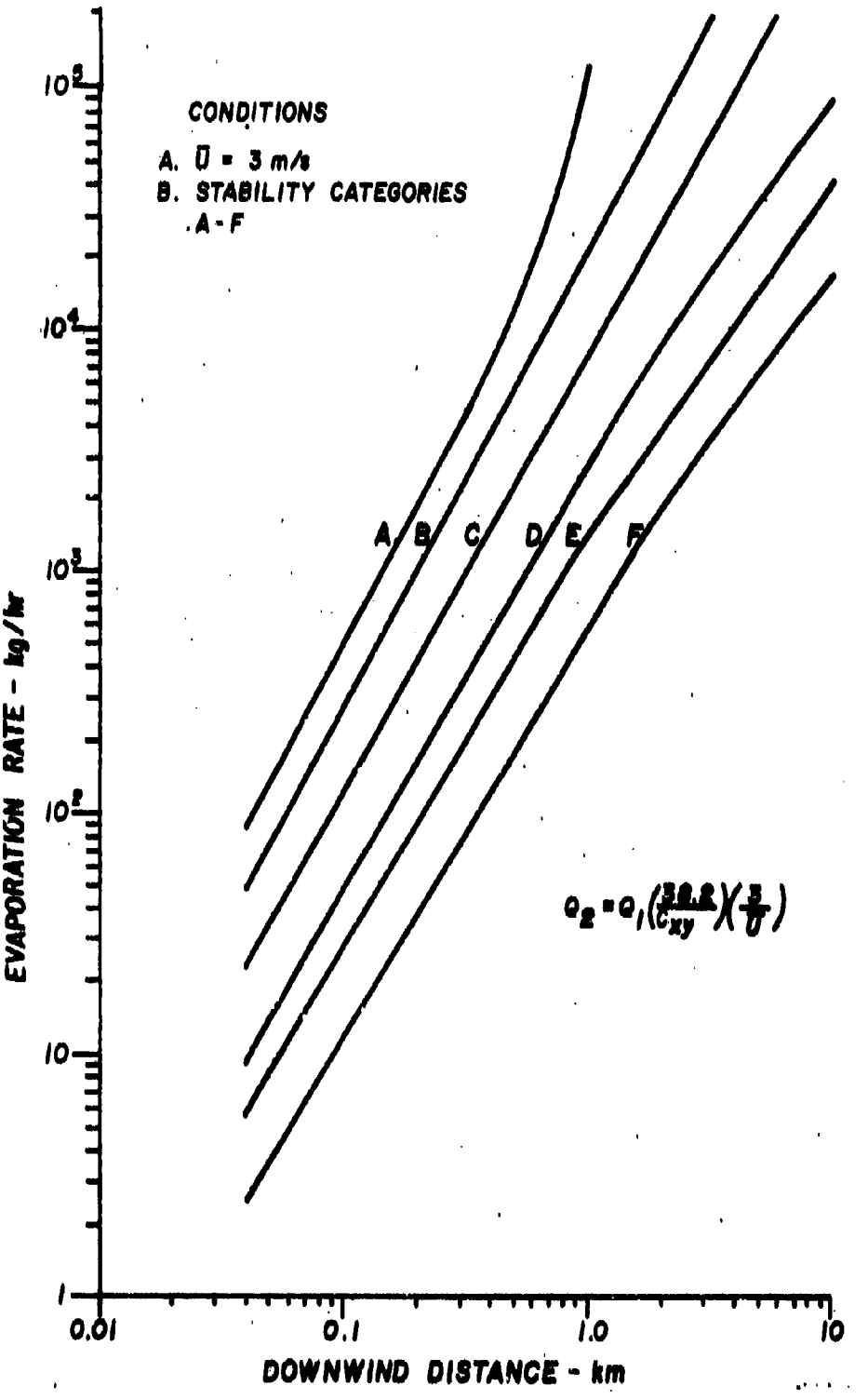

Figure 19. Downwind Evacuation Distance to the Short-Term Public Exposure Limit Concentration for UDMH.

3. Comparison of Hand Calculated Downwind Dispersion Data with EPA PTDIS MOdel

The downwind concentration data graphically illustrated in the previous section were hand-calculated using dispersion algorithms from Turner's Workbook of Atmospheric Dispersion Estimates (Reference 7). This hand-calculated data was then compared to computer generated concentration data, for identical spill and meteorological conditions, using the EPA point-distance (PTDIS) dispersion program (Reference 9). The EPA computer program verified the accuracy of the hand-calculated dispersion data and the resulting graphs.

PTDIS is one of three steady-state Gaussian plume point source models that have recently been added to EPA's UNAMAP (User's Network for Applied Modeling of Air Pollution) system. The model determines the variation of ground-level concentration with downwind distance and the crosswind distance to a selected isopleth concentration. Program input parameters include source strength, effective height of emission, physical stack height, stack gas temperature stack volume flow, gas velocity, ambient air temperature, stability class, wind speed and mixing height. Concentration values for up to 50 downwind distances may be computed for any source strength. An isopleth option may be called which calculates the half-width to a specified exposure limit. The model assumes no topographic obstructions in the vicinity of the source and that the terrain is flat or gently rolling.

SECTION V

CONCLUSIONS AND RECOMMENDATIONS

Propellant evaporation and dispersion models have been developed for hydrazine, MMH and UDMH propellant ground spills. The evaporation model computes the rate of propellant evaporation as a function of ground temperature, solar insolation, air temperature, wind speed and spill dimensions. This model will significantly improve predictions of hazard zones resulting from propellant spills. Results can be an order of magnitude different than those obtained using models that do not consider heat gain and losses to the evaporating pool.

Sensitivity analyses of the evaporation input parameters indicate that spill area, ground temperature, ground roughness and propellant type are important factors for consideration. Medium sensitive evaporation input parameters include wind speed, air temperature, ground temperature (when T_G is less than T_p) and mid-day solar insolation. Spill depth and atmospheric emissivity were found to be the least sensitive in the evaporation program.

A simple Gaussian dispersion model is presented and applied to a sample problem to calculate the peak downwind, ground-level concentration and the crosswind distance to the 7, 2.8 and 38.2 mg/m^3 STPL. This resulted in hazard corridors reaching 480, 1380, and 680 meters downwind of a 36,000 liter railcar spill at an ambient air temperature of 15°C for N_2H_4, MMH and UDMH respectively. Downwind hand-calculated concentration predictions were verified and found to agree with the EPA point-distance (PTDIS) computer model.

Three follow-on projects are recommended. The evaporation of propellant mixtures needs to be addressed. Titans use a 50 percent mixture of hydrazine and UDMH (Aerozene 50) and the F-16 uses a 70 percent mixture of hydrazine in water. Comparison with experimental laboratory data indicate that the model predicts only the initial, first hour average evaporation rate. The parameters that describe the transient propellant evaporation rate as a function of time and humidity, need to be defined. Finally, atmospheric photochemical reaction or decomposition of hydrazine propellants require further investigation.

REFERENCES

1. Environmental Fate of Hydrazine Fuels, USAF Space and Missile Systems Organization TN-SAMSO-AFCEC-2109-76-45, January 1976.

2. Watje, W., "Potential of a Hydrazine Type Spill or Emission During Movement from Supplier to User", Presented at the Conference of Environmental Chemistry of Hydrazine Fuels, Tyndall AFB, CEEDO TR 78-14, 13 Sep 77.

3. Mackay, D. and Matsugo, R. S., "Evaporation Rates of Liquid Hydrocarbon Spills on Land and Water", Can J Ch Eng, 51 pp. 434-439, 1973.

4. Eyl, A. et al, "Control and Treatment of Small Hydrazine Spills", CEEDO-TR-78-12, 1978.

5. Slade, D. H. (editor), Meteorology and Atomic Energy 1968, TID-24190, National Technical Information Service, US Department of Commerce, Springfield, Virginia 1968.

6. Schulze, R. H., Notes on Dispersion Modeling, Dispersion Modeling Workshop, Trinity Consultants, Sep 9, 1977.

7. Turner, D. B., Workbook of Atmospheric Dispersion Estimates, Technical Information and Publications, Office of Air Programs, Publication No. AP-26, Environmental Protection Agency, Research Triangle Park, NC 1970.

8. Guide For Short Term Exposures Of The Public To Air Pollutants, V. Guide for Hydrazine, Monomethylhydrazine, and 1,1-Dimethylhydrazine, by The Committee on Toxicology of the National Academy of Sciences - National Research Council, Washington, DC January 1975.

9. Khanna, S. B., Handbook for UNAMAP, Walden Division of ABCOR Inc., Mar 1976.

10. Perry, R. H., and Chilton, C. H., (editors) Chemical Engineers' Handbook, 5th Edition, McGraw-Hill Book Company, 1973.

11. Chemical Rocket/Propellant Hazards, Volume II, Liquid Propellants, AFM 161-30, 10 April 1973.

12. Bird, R. B., Stewart, W. E. and Lightfoot, E. N. Transport Phenomena, John Wiley & Sons Inc., New York, 1966.

13. Perry, R. H., et al (editors), Chemical Engineers' Handbook, 4th Edition, McGraw-Hill Book Company, New York, 1963.

14. Schmidt, E., and Silveston, P. L., "Natural Convection in Horizontal Layers", Heat Transfer, Vol 55(29), American Institute of Chemical Engineers, Chicago, 1959.

15. Sutton, O. G., Micrometeorology, McGraw-Hill Book Company, Inc., New York, 1953.

APPENDIX A

EMISSION COMPUTATION

The evaporation of a liquid pool can be related to the concentration driving force and the mass transfer rate constant by the following equation:

$$Q_M = k_m (C_1 - C_A) \qquad \text{(A-1)}$$

where

Q_M = mass transfer rate, kmoles/hr-m^2

k_m = vapor phase mass transfer rate coefficient, m/hr

C_1 = propellant vapor concentration at the liquid pool interface, kmoles/m^3

C_A = propellant vapor concentration in the bulk atmosphere, assumed zero.

The computation assumes ideal gas behavior of the propellant vapor across the diffusing film. The concentration term (C_1) can be expressed, according to the ideal gas law, in vapor pressure as follows:

$$M/V = C_1 = P_v/RT_p \qquad \text{(A-2)}$$

and

$$Q_M = k_m P_v/R(T_p + 273) \qquad \text{(A-3)}$$

where

P_v = vapor pressure of the spilled liquid kN/m^2 = kPa

R = universal gas constant, 8.314 kPa-m^3/kmole · ^oK

T_p = temperature of the evaporating propellant liquid, ^oC

M = number of moles of propellant, kmoles

V = volume of propellant vapor, m^3

The mass transfer coefficient (k_m) is computed from the following equation: (Reference 3)

$$k_m = CU^{(2-n)/(2+n)} x^{(-n)/(2+n)} \qquad \text{(A-4)}$$

where

k_m = mass transfer coefficient, m/hr

C = dimensionless constant and a function of the Schmidt number

$\bar{U}$ = wind speed at a height of 10m, m/hr

n = a function of the atmospheric lapse rate

X = diameter of spill, m

For average atmospheric conditions, a value of n = 0.25 is reasonable (Reference 3). The constant C is calculated for any propellant using the following equation (Reference 3):

$$C = 0.0292\ Sc^{-0.67} \qquad \text{(A-5)}$$

where

Sc = Schmidt number = $\mu_{FM}/\rho_{FM}D_v$

μ_{FM} = viscosity of the air-propellant mixture in the stagnant film, g/cm-sec

ρ_{FM} = density of the air-propellant mixture in the stagnant film, g/cm^3

D_v = diffusivity, cm^2/sec

The Schmidt number is a dimensionless number and a function of the viscosity and density of the air-hydrazine mixture in the stagnant film and the diffusivity of the propellant fuel in air. The viscosity of the air-hydrazine vapor mixture is based on the pure component viscosities of the air and propellant vapors in the diffusing film. The viscosity of a pure vapor is calculated from the following equation: (Reference 10)

$$\mu_{FP} = \frac{2.7\ (MW_p)^{1/2}\ \ (T_F + 273)^{3/2}}{V_o 2/3\ (T_F + 1.47\ T_b + 674.31)\ 10^6} \qquad \text{(A-6)}$$

where

μ_{FP} = viscosity of the pure gas component, g/cm-sec or poise

MW_p = molecular weight of the propellant.

T_F = temperature of the stagnant vapor film
= $(T_A + T_p)/2$, °C

T_A = temperature of the air, °C

T_b = boiling point temperature of propellant liquid, °C

V_o = volume of the propellant liquid at its boiling point, cc/g-mole

The viscosity of a propellant vapor as a function of temperature can be represented by the following general equation: (Reference 10)

$$\mu = \frac{K(T_F)^{3/2}}{T_F + 1.47\ T_b} \qquad \text{(A-7)}$$

where

K = constant for any specific gas

T_b = boiling point temperature, °K

A general equation for the viscosity of air as a function of temperature can be computed by looking up a reference viscosity value at temperature T_F, and calculating the constant K from equation A-7. Based on this, the following equation for viscosity of air was developed:

$$\mu_{FA} = 1.45\ (10^{-5})\ \frac{T_F^{3/2}}{T_F + 116} \qquad \text{(A-8)}$$

The viscosity of the vapor mixture in the stagnant film (μ_{FM}) is computed from the following equation: (Reference 10)

$$\mu_{FM} = \frac{Y\ \mu_{FP}\ (MW_p)^{1/2} + (1 - Y)\ \mu_{FA}\ (MW_A)^{1/2}}{Y(MW_p)^{1/2} + (1 - Y)\ (MW_A)^{1/2}} \qquad \text{(A-9)}$$

where

μ_{FM} = viscosity of the air-propellant mixture, poise

Y = average mole fraction of the propellant vapor = $P_v/2P_T$

P_v = vapor pressure of the pure propellant vapor, kPa

P_T = barometric pressure, = 101.3 kPa

μ_{FP}, μ_{FA} = viscosity of the pure film components, propellant, air respectively, poise

MW_p, MW_A = molecular weight of propellant, air, respectively

To solve equation A-9, the vapor pressures (P_v) of the pure gas components, as a function of the pool temperature (T_p), is required. The following equations, modified for unit consistency, are presented: (Reference 11)

N_2H_4

$$\log P_v = -7.38113 - \frac{653.880}{T_p + 273} + 0.047914\ (T_p + 273) \qquad \text{(A-10)}$$

$$-4.98860\ (10^{-5})\ (T_p + 273)^2$$

MMH

$$\log P_v = 6.23648 - \frac{1104.571}{T_p + 273} - \frac{152227.6}{(T_p + 273)^2} \qquad \text{(A-11)}$$

UDMH

$$\log P_v = 5.84068 - \frac{875.89}{T_p + 273} - \frac{140001.1}{(T_p + 273)^2} \qquad \text{(A-12)}$$

The density (ρ_{FM}) of the air-propellant mixture in the stagnant film must also be determined to evaluate the Schmidt number. The density of the gas mixture is represented by the following equation:

$$\rho_{FM} = \frac{\overline{MW}\ P_T}{R'\ T_F} \qquad \text{(A-13)}$$

where

$\overline{MW}$ = molecular weight of the propellant-air mixture, $= YMW_p+(1-Y)MW_A$

R' = universal gas constant, 8314 kPa-cm^3/gmole - ^oK

Finally, an estimate of the diffusivity, D_v, across the gas film is determined from the following equation: (Reference 12)

$$D_v = \frac{0.0018583 \left[T_F^3\ (1/MW_A + 1/MW_p)\right]^{1/2}}{P_T \qquad r_{A-P}^2 \qquad \Omega_{A-P}} \qquad \text{(A-14)}$$

where

D_v = diffusivity, cm^2/sec

$r_{A-P} = (r_A + r_p)/2$

r_A, r_p = collision diameter of the air-propellant molecules, Angstroms

Ω_{A-P} = collision integral and a function of kT_F/ε_{A-P}

k = Boltzman constant, $1.38(10^{-6})$ ergs/molecule-^oK

ε_{A-P} = energy of molecular interaction, ergs

The collision integral, Ω_{A-P}, can be determined by calculating first the (ε_{A-P}/k) force constant for each gas pair as follows: (Reference 13)

$$\frac{kT_F}{\varepsilon_{A-P}} = T_F\left[\left(\frac{k}{\varepsilon_A}\right)\left(\frac{k}{\varepsilon_p}\right)\right]^{1/2} \qquad \text{(A-15)}$$

For air, $\varepsilon_A/k = 97^{\circ}K$. For the propellants, ε_p/k was calculated from the following equation: (Reference 13)

$$\varepsilon_p/k = 1.15(T_b + 273) \qquad \text{(A-16)}$$

where T_b is the boiling point temperature of the propellant in $^{\circ}C$.

Based on tabular values of kT_F/ε_{A-P} for the temperature range of $-31^{\circ}C$, to $59^{\circ}C$ a general regression formula for the collision integral (Ω_{A-P}) as a function of temperature was developed:

$$\log \Omega_{A-P} = -0.43 \log\left(\frac{k}{\varepsilon_{A-P}} T_F\right) + 0.15 \qquad \text{(A-17)}$$

The following specific equations were developed for the three propellants under consideration:

$\underline{N_2H_4}$ $\quad \log \Omega_{A-P} = -0.43 \log (T_F + 273) + 1.15 \qquad$ (A-18)

$\underline{MMH}$ $\quad \log \Omega_{A-P} = -0.43 \log (T_F + 273) + 1.14 \qquad$ (A-19)

$\underline{UDMH}$ $\quad \log \Omega_{A-P} = -0.43 \log (T_F + 273) + 1.13 \qquad$ (A-20)

To calculate the average collision diameter, (r_{A-P}) required in equation A-14, the collision diameters of the component gas species are calculated as follows: (Reference 13)

$$r_p = 1.18(V_o)^{1/3} \qquad \text{(A-21)}$$

where V_o = volume of the liquid at the normal boiling point,

cc/g-mole

The collision diameter for air, r_A, is given as 3.617A (Reference 13). V_o is calculated by dividing the density of the propellant, at its boiling point, into the molecular weight of the propellant. The density of a liquid at its boiling point is computed by the following equation: (Reference 10)

$$\rho_{LB} = \rho_{L1}\left(\frac{T_C - T_b}{T_C - T_{L1}}\right)^{1/3} \qquad \text{(A-22)}$$

where

ρ_{LB} = density of the liquid at its boiling point, g/cc
N_2H_4 - 0.911, MMH - 0.801, UDMH - 0.740

ρ_{LI} = density of the liquid at T_{L1}, g/cc

T_b = temperature of a liquid at its boiling point, °C

T_c = critical temperature of the propellant, °C

T_{L1} = any propellant temperature where density is known.

Equation A-3 can now be solved, assuming a tentative pool temperature, T_p. The pool temperature of an evaporating pool may not equal the temperature of the air. To determine the steady-state pool temperature (T_p), a heat balance analysis of the evaporating pool system must be performed. The following parameters define the heat-balance equation: (Reference 3)

$$Q_G + Q_H + Q_S + Q_A = Q_E + H_E \qquad \text{(A-23)}$$

where

Q_G = convective heat transfer from the soil or surface to the pool, J/hr

Q_H = convective heat transfer from the atmosphere, J/hr

Q_S = solar insolation, J/hr

Q_A = radiative heat gain from the atmosphere, J/hr

Q_E = radiative heat loss from the liquid pool, J//hr

H_E = evaporative heat loss from the pool, J/hr

Heat transfer from the ground to the liquid pool (Q_G) is based on experimental heat transfer studies through a horizontal layer bounded on the top by a cold surface and on the bottom by a heated surface.

The Rayleigh number (N_{RA}), (Grashof number (N_{GR}) times the Prandtl Number (N_{PR})) is correlated with the Nusselt number for five distinct modes of heat transfer. The five modes are defined as follows:

a. $100 < N_{RA} < 1700$ $\quad N_{NU} = 1$. Heat transfer is by conduction only and the fluid remains immobile.

b. $1700 < N_{RA} < 3000$ $\quad N_{NU} = 0.0012\ N_{RA}^{0.90}$ This mode defines the critical condition where creeping convection begins. The fluid begins to circulate and heat transfer is by conduction and convection.

c. $3000 < N_{RA} < 8000\ N_{PR}^{0.2}$ $\quad N_{NU} = 0.24\ N_{RA}^{0.25}$ This heat transfer mode is defined as laminar convection and is described by uniform heat flow contours.

d. $8000\ N_{PR}^{0.2} < N_{RA} < 18000\ N_{PR}^{0.2}$ $\quad N_{NU} = 0.3\ N_{GR}^{0.16} N_{PR}^{0.21}$

This region is defined as the transitional phase where heat convection changes from laminar to turbulent convection.

e. $N_{RA} > 18000\ N_{PR}^{0.2}$ $\quad N_{NU} = 0.10 N_{GR}^{0.31} N_{PR}^{0.36}$

This region is characterized by turbulent convective heat transfer from the ground to the liquid pool.

The heat transfer from the ground to the liquid pool is described by the following equation:

$$Q_G = h_g (T_G - T_p) A_p \qquad \text{(A-24)}$$

where

h_g = heat transfer coefficient from ground to liquid pool, $J/m^2 \cdot hr \cdot {}^oK$

T_G, T_p = temperature of the ground and pool, respectively, ${}^oK$

A_p = area of the liquid evaporating pool, m^2

The heat transfer coefficient can be calculated from the following equation: (Reference 14)

$$h_g = \frac{k_L \, A \, N_{GR}^{\ B} \, N_{PR}^{\ C}}{L} \qquad \text{(A-25)}$$

where

k_L = thermal conductivity of the liquid J/m·hr·°K

A, B, C = constants whose value depend upon the five distinct modes of heat transfer that can occur.

N_{GR} = Grashof number = $g \, \beta \, L^3 \, \rho_L^2 / \mu_L^2$

β = ratio of volume change to mean volume per degree change in temperature, 1/°K

L = liquid layer thickness, meters

g = gravitational constant = 1.27×10^8 m/hr^2

ρ_L = liquid density, kg/m^3

μ_L = liquid viscosity, kg/m·hr

N_{PR} = Prandtl number = $\frac{C_L \, \mu_L}{k_L}$

Depending on the heat transfer mode, values of A, B, C are assigned. For instance, when $T_G < T_P$, heat transfer to the ground is by conduction and A = 1, and B = C = 0. Equation A-25 then simplifies as follows:

$$h_g = \frac{k_L}{L} \qquad \text{(A-26)}$$

For this case the heat transfer rate is inversely proportional to the pool depth. When $T_G > T_P$ and heat transfer is by turbulent convection, A = 0.1, B = 0.31 and C = 0.36. For this case, Equation A-25 looks as follows:

$$h_g = \frac{k_L \, 0.1 \, N_{GR}^{\ 0.31} \, N_{PR}^{\ 0.36}}{L} \qquad \text{(A-27)}$$

Since N_{GR} is a function of L^3, pool depth cancels out in the above equation and becomes an insensitive parameter in the heat transfer equation.

The heat transfer from the atmosphere to the evaporating pool is described by the following equation: (Reference 3)

$$Q_H = h(T_A - T_p)A_p \qquad \text{(A-28)}$$

h = heat transfer coefficient, J/m2·hr·°K

h is further defined as: (Reference 3)

$$h = k_m \rho_{FM} C_{PFM} (Sc/P_R)^{0.67} \qquad \text{(A-29)}$$

where

ρ_{FM} = density of the film vapor mixture, g/m^3. For unit consistency, multiply the density in g/cc by 10^6.

C_{PFM} = heat capacity of film vapor, J/g·°K

Equation A-29 is modified as shown below for dimensional consistency:

$$h = k_m \, 10^6 \, \rho_{FM} C_{PFM} (Sc/P_R)^{0.67} \qquad \text{(A-30)}$$

The heat capacity of the air-propellant vapor mixture in the film is calculated first for each pure component vapor as follows: (Reference 13)

N_2H_4 (A-31)

$$C_{PFP} = \left[0.357 + 7.919(10^{-4})(T_F + 273) + 2.44(10^{-7})(T_F + 273)^2\right]4.19$$

MMH (A-32)

$$C_{PFP} = \left[8.49(10^{-2}) + 9.88(10^{-4})(T_F + 273) - 3.22(10^{-7})(T_F + 273)^2\right]4.19$$

UDMH (A-33)

$$C_{PFP} = \left[6.32(10^{-2}) + 1.087(10^{-3})(T_F + 273) - 3.63(10^{-7})(T_F + 273)^2\right]4.19$$

where

C_{PFP} = heat capacity of the pure propellant vapor, J/g·°K

T_F = temperature of the film, °C

Air

$$C_{PFA} = \left[0.232 + 1.622(10^{-5})\ (T_F + 273) + 3.96(10^{-8})\ (T_F + 273)^2\right] 4.19 \qquad \text{(A-34)}$$

where

C_{PFA} = heat capacity of air, J/g·°K

The heat capacity of the propellant-air mixture is represented by the following equation:

$$C_{PFM} = \frac{Y(C_{PFP})\ (MW_P) + (1 - Y)\ (C_{PFA})\ (MW_A)}{(Y)\ (MW_P) + (1 - Y)\ (MW_A)} \qquad \text{(A-35)}$$

The Prandtl number, also required in equation A-30, is defined by the following expression:

$$P_R = \frac{C_{PFM}\ (\mu_{FM})\ 3.6(10^5)}{k_{FM}} \qquad \text{(A-36)}$$

where

P_R = Prantl number, dimensionless

C_{PFM} = heat capacity of the vapor film mixture, J/g·°K

μ_{FM} = viscosity of the vapor film mixture, g/cm·sec

k_{FM} = thermal conductivity of the film mixture, J/hr·m·°K

$3.6(10^5)$ = conversion factor to change g/cm·sec to g/m·hr

The thermal conductivity (k_{FP}) of the pure propellant vapor is computed from the following equation: (Reference 13)

$$k_{FP} = 3.6(10^5)\ \mu_{FP}\left(C_{PFP} + \frac{2.48}{MW_P}\right) \qquad \text{(A-37)}$$

where

k_{FP} = thermal conductivity of the pure propellant vapor, J/hr·m·°K

μ_{FP} = viscosity of the propellant, g/cm·sec

C_{PFP} = heat capacity of vapor, J/g·°K

For air, the thermal conductivity (k_{FA}) is expressed by an equation that assumes a straight-line relationship between k_{FA} at 0°C and 100°C:

$$k_{FA} = 87.184 + (T_F)\ 0.2679 \qquad \text{(A-38)}$$

where

k_{FA} = thermal conductivity of air, J/hr·m·°K

T_F = temperature of the film, °C

The thermal conductivity of the air-propellant mixture is represented by the following equation: (Reference 13)

$$k_{FM} = \frac{Y\ k_{FP}\ (MW_P)^{1/3} + (1 - Y)\ k_{FA}\ (MW_A)^{1/3}}{Y\ (MW_P)^{1/3} + (1-Y)\ (MW_A)^{1/3}} \qquad \text{(A-39)}$$

The heat input to the pool due to solar radiation is described by the following equation: (Reference 3)

$$Q_s = (1-a)\ R_s A_p \qquad \text{(A-40)}$$

where

Q_s = incident solar radiation, J/hr

a = surface albedo, the radiation that is reflected from the pool

R_s = solar radiation, J/m^2·hr

The albedo, is tentatively selected as 0.14 which is in reasonable agreement with the generally accepted values for water surfaces. (Reference 3).

The radiative heat input to the propellant pool due to counter-radiation from the atmosphere is represented by the following equation: (Reference 3)

$$Q_A = e_a S(Ta + 273)^4 A_p \qquad \text{(A-41)}$$

where

Q_A = radiative heat gain from the atmosphere, J/hr

e_a = emissivity of the atmosphere

S = Steffan-Boltzmann constant, $2.042(10^{-4})$ $J/m^2 \cdot hr \cdot {}^oK^4$

The emissivity of the atmosphere is primarily a function of the water vapor pressure and tentatively assumed constant at 0.75 (Reference 3).

The radiative heat loss from the pool to the atmosphere is presented by the following equation: (Reference 3)

$$Q_E = e_p S(T_p + 273)^4 A_p \qquad \text{(A-42)}$$

where

Q_E = heat loss from the pool, J/hr

e_p = emissivity of the pool

The emissivity for water, equal to 0.95, is tentatively used until specific values for the hydrazine family can be obtained.

Finally, the heat loss from the pool due to evaporation can be expressed by the following equation: (Reference 3)

$$H_E = \frac{k_m A_p MW \lambda_p P_V}{R(T_p + 273)} \qquad \text{(A-43)}$$

where

H_E = evaporative heat loss from the pool, J/hr

k_m = vapor mass transfer rate coefficient, m/hr. See equation A-4.

λ_p = enthalpy of vaporization at the equilibrium pool temperature, J/kg

Using Watson's Correlation, λ_p can be computed from the following expression: (Reference 13)

$$\lambda_p = \lambda_\omega \left(\frac{T_c - T_p}{T_c - T_1} \right)^{0.38} \qquad \text{(A-44)}$$

where

T_c = critical temperature of the propellant, °C

λ_1 = reference enthalpy of vaporization at T_1

The critical temperatures for the three liquid propellants are as follows: N_2H_4 - 380°C; MMH - 312°C; UDMH - 250°C. The reference enthalpy of vaporization (λ_1) used in the sample calculations are as follows: N_2H_4 - $1.36(10^6)$ J/kg at T_1 = 25°C; MMH - $8.75(10^5)$ J/kg at T_1 = 25°C; UDMH - $5.44(10^5)$ J/kg at T_1 = 62.5°C.

A value of T_p is assumed and equations A-24 to A-44 are solved to determine if the equality condition set by equation A-23 has been met. Successive iterations are made until $T_p \pm 0.1$ are calculated. This value is subsequently used in equation A-45 to calculate the mass flux of propellant evaporating into the atmosphere.

$$Q_M = k_m P_v (MW) A_p / R\, T_p \qquad \text{(A-45)}$$

where

Q_M = Emission rate from the pool, kg/hr

APPENDIX B

1. Flow Chart
2. Computer Definitions
3. Listing of Computer Code

APPENDIX B

EVAPORATION PROGRAM FLOW-CHART

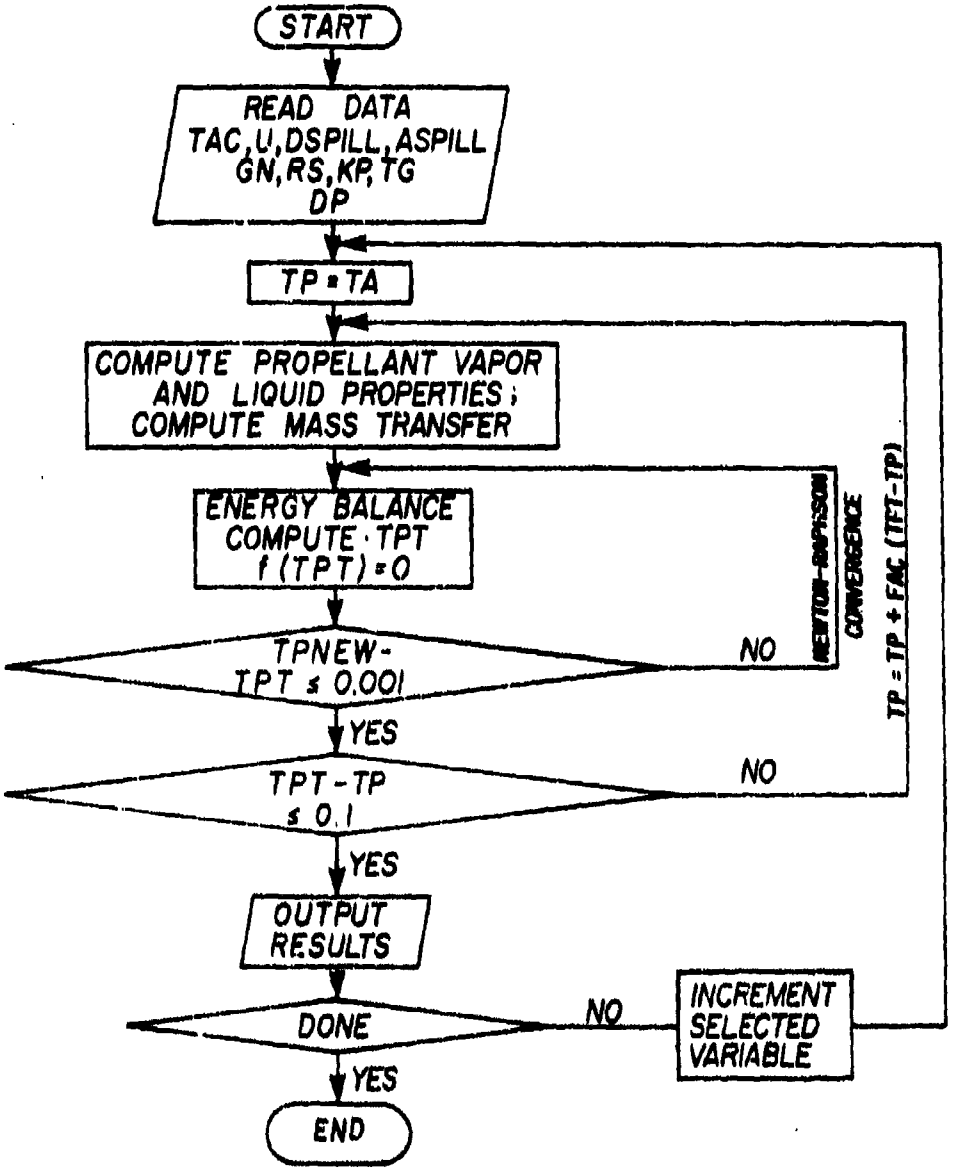

```
C         EVAP -- HYDRAZINE EVAPORATION PROGRAM
          COMMON TAC,U,DSPILL,ASPILL,GN,RS,KP,TG,DP
          CALL ERASE
          CALL EVAPIN
          FAC=.2
          ZIP=.001
          EA=.75
          TG=TG+273.
          DO 36 IJ=1,20
          IF(KP-2)100,200,300
C  KP=1 FOR HYDRAZINE
  100     WMOL=32.
          CPA=.357
          CPB=7.919
          CPC=2.44
          VO=35.13
          TBOIL=387.4
          OMEGK=1.15
          HVAP1=3.24E5
          TVAP=298.
          ALB=.14
          EP=.95
          TCP=653
          GO TO 400
C  KP=2 FOR MONOMETHYL HYDRAZINE
  200     WMOL=46.
          CPA=.0849
          CPB=9.88
          CPC=-3.22
          VO=57.43
          TBOIL=360.7
          OMEGK=1.14
          HVAP1=2.09E5
          TVAP=298.
```

```
            TVAP=293.
            ALB=.14
            EP=.95
            TCP=585.
            GO TO 400
C  KP=3 FOR UNSYM. DIMETHYL HYDRAZINE
 300        WMOL=60.
            CPA=.0632
            CPB=10.87
            CPC=-3.62
            VO=81.28
            TBOIL=335.47
            OMEGK=1.13
            HVAP1=1.3E5
            TVAP=335.5
            ALB=.14
            EP=.95
            TCP=523.
 400        RBAR=(3.617+1.18*VC**.333)/2.
            PT=101.3
            TA=TAC+273.
            TP=TA
            TF=TA
            DO 13 I=1,100
            TM=(TP+TG)/2.
            IF (KP-2)26,27,28
 26         VPF=-653.88/TP+.047914*TP-4.9886E-5*TP**2
            DENL=1230.78-.62668*TM-4.5204E-4*TM**2
            BETA=8.9E-4
            TCONL=75.84+2.359*TM-4.824E-3*TM**2
            CPL=295.12+2.0193*TM-1.8539E-3*TM**2
            VISL=10.**(2.6225-.015384*TM+1.5395E-5*TM**2)
            VPP=10**(-7.38113+VPF)
            GO TO 29
 27         VPP=10**(6.23648-1184.571/TP-152227.6/TP**2)
```

```
      CPL=652.8-.017284*TM+5.9142E-4*TM**2
      VISL=10.**(-8.55070+6123.96/TM-1.7458E6/TM**2+1.8509E8/TM**3)
      DENL=1150.34-0.93949*TM
      BETA=1.084E-3
      TCONL=122.49+.792*TM-1.636E-3*TM**2
      GO TO 29
28    UPP=10**(5.86068-875.89/TP-140001./TP**2)
      DENL=1060.41-.77507*TM-4.8648E-4*TM**2
      VISL=1.00.**(-.810410-623.532/TM+181151.8/TM**2)
      BETA=1.361E-3
      CPL=407.1+.8838*TM
      TCONL=244.71-.3667*TM
29    CONTINUE
      CPP=CPA+CPB*1.E-4*TF+CPC*1.E-7*TF**2
      VISP=(27.*WMOL**.5*TF**1.5/(VO**.67*(TF+1.47*TBOIL)))/1.E6
      TCONP=(CPP+2.48/WMOL)*VISP*3.6E5
      HCA=.232+1.622E-5*TF+3.96E-8*TF**2
      TCONA=.06398*(TF-273.)+20.829
      VISA=1.45E-5*(TF**1.5/(TF+116.))
      OMEGA=10.**(-.43*(ALOG(TF)/2.30259)+OMEGK)
      DV1=.0018583*TF**1.5*(.03448+1./WMOL)**.5
      DV2=RBAR**2*OMEGA*PT/101.3
      DV=DV1/DV2
      Y=UPP/(2.*PT)
      VISFD=WMOL**.5*Y+5.385*(1.-Y)
      VISFN=Y*VISP*WMOL**.5+(1.-Y)*VISA*5.385
      VISFM=VISFN/VISFD
      DENFM=(WMOL*Y+29.*(1.-Y))*PT/(8314.4*TF)
      CPFLN=Y*CPP*WMOL+(1.-Y)*HCA*29.
      CPFLD=Y*WMOL+(1.-Y)*29.
      CPFLM=CPFLN/CPFLD
      TCOFD=Y*WMOL**.333+3.072*(1.-Y)
      TCOFN=Y*TCONP*WMOL**.33+(1.-Y)*3.072*TCONA
      TCOFM=TCOFN/TCOFD
      SC=VISFM/(DENFM*DV)
```

```
      PR=CPFLM*VISFM*3.6E5/TCOFM
      HVAPO=HVAP1*((TCP-TP)/(TCP-TVAP))**.38
      TRK1=(.0292/SC**.667)*(U*3600.)**((2.-GN)/(2.+GN))
      TRK2=DSPILL**(-GN/(2.+GN))
      TRK=TRK1*TRK2
      FM=WMOL*TRK*VPP/(8.3144*TP)
      H=1.E6*TRK*DENFM*CPFLM*(SC/PR)**.667
      CONST=(1.-ALB)*RS+4.878E-5*EA*TA**4-FM*HVAPO
      TPT=TP
      DO 14 II=1,100
20    GR=1.27E8*BETA*DP**3*DENL**2/VISL**2
      PRL=CPL*VISL/TCONL
      RA=GR*PRL
      IF(TG-TPT)41,41,21
21    IF(GR*PRL-1700.)41,41,42
C     CONDUCTION REGION
41    A=1
      B=0
      C=0
      GO TO 25
42    IF(GR*PRL-3000.)43,43,44
C     CREEPING REGION
43    A=.0812
      B=.9
      C=.9
      GO TO 25
44    IF(GR*PRL-8000.*PRL**.2)45,45,46
C     LAMINAR REGION
45    A=.24
      B=.23
      C=.25
      GO TO 25
46    IF(GR*PRL-18000.*PRL**.2)47,47,48
C     TRANSITION REGION
47    A=.3
```

```
            B=.16
            C=.21
            GO TO 25
C           TURBULENT REGION
48          A=1
            B=.31
            C=.36
25          HG=A*GR**B*PRL**C*TCONL/DP
 18         TPT1=H*(TA-TPT)+HG*(TG-TPT)
            TPT2=-4.878E-5*EP*TPT**4+CONST
            PRIM=-H-HG-1.854E-4*TPT**3
            TPNEW=TPT-(TPT1+TPT2)/PRIM
            CRIT=ABS(TPNEW-TPT)
            TPT=TPNEW
            IF(CRIT-.001)114,114,14
 14         CONTINUE
 114        CONTINUE
            DEL=TPT-TP
            IF(ABS(DEL)-ZIP)113,15,15
 15         TP=TP+FAC*DEL
 13         TF=(TA+TP)/2.
 113        VAPRT=FM*ASPILL
            CALL EVOUT
            KP=KF+1
36          CONTINUE
            CALL EXIT
            END
```

```
C       EVAPIN -- INPUT FOR "EVAP"
        SUBROUTINE EVAPIN
        COMMON TAC,U,DSPILL,ASPILL,GN,RS,KP,TG,DP,H,HG,TA,TPT,
        1 TP,ALB,EA,EP,FM,HUAPO,VAPRT,RA
        WRITE(1,1003)
        WRITE(1,1004)
        READ(1,3)TAC
        WRITE(1,1002)
        READ(1,3)U
        WRITE(1,1005)
        READ(1,3) DSPILL
        WRITE(1,1006)
        READ(1,3) ASPILL
        WRITE(1,1007)
        READ(1,3)GN
        WRITE(1,1008)
        READ(1,3)RS
        WRITE(1,1009)
        READ(1,5)KP
        WRITE(1,1012)
        READ(1,3)TG
        WRITE(1,1013)
        READ(1,3)DP
        CALL ERASE
        WRITE (1,2)
1003    FORMAT(1X,'INPUT THE FOLLOWING DATA:')
1004    FORMAT(1X,'AIR TEMPERATURE IN CELCIUS')
1002    FORMAT(1X,'WIND VELOCITY IN METERS PER SECOND')
1005    FORMAT(1X,'SPILL DIAMETER IN METERS')
1006    FORMAT(1X,'SPILL AREA IN SQ METERS')
1007    FORMAT(1X,'GRND ROUGHN FAC')
1008    FORMAT(1X,'SOLAR RATE, CAL/SQ M HR')
1009    FORMAT(1X,'LIQ TYPE; HYD=1, MMH=2, UDMH=3')
1012    FORMAT(1X,'GRND TEMP IN C')
```

```
1013    FORMAT(1X,'DEPTH OF POOL IN METERS')
  3     FORMAT (F7.0)
    5   FORMAT (I2)
2       FORMAT(2X,'TA',6X,'TG',6X,'TP',7X,'SUN',8X,'WIND',
       1 4X,'RATE'/)
        RETURN
        END
```

```
C       EVOUT -- OUTPUT FOR "EVAP"
        SUBROUTINE EVOUT
        COMMON TAC,U,DSPILL,ASPILL,GN,RS,KP,TG,DP,H,HG,TA,TPT,
        1 TP,ALB,EA,EP,FM,HVAPO,VAPRT,RA
        WRITE(1,1)TA,TG,TP,RS,U,VAPRT
1       FORMAT(2(F5.1,2X),F11.7,2X,E11.4,2X,F5.1,2X,F9.3)
        QH=H*(TA-TPT)*ASPILL
        QG=HG*(TG-TPT)*ASPILL
        QS=(1.-ALB)*RS*ASPILL
        QA=4.878E-5*EA*TA**4*ASPILL
        QE=4.878E-5*EP*TPT**4*ASPILL
        HE=FM*HVAPO*ASPILL
        WRITE(1,10)RA,QH,QG,QS,QA,QE,HE
10      FORMAT(4(E11.3,2X),/,3(E11.3,2X))
        RETURN
        END
```

LIST OF SYMBOLS

COMPUTED TERMS IN EVAP PROGRAM

Computed Variables		Variable Description
Technical Report	Computer Program	
A, B, C,	A, B, C,	Constants used in generalized heat transfer correlation equation, $N_{NU} = A\ N_{GR}^{B}\ N_{PR}^{C}$.
β	Beta	The ratio of volume change to mean volume per degree change in temperature, $1/^{o}K$
$Q_S+Q_A-H_E$	CONST	Solar insolation + radiative heat gain from the atmosphere - evaporative heat loss, J/hr
C_L	CPL	Liquid heat capacity, $J/kg\cdot^{o}K$
C_{PFM}	CPFLM	Heat capacity of the propellant-air mixture $J/g\cdot^{o}K$
C_{PFP}	CPP	Heat capacity of pure propellant vapor, $J/g\cdot^{o}K$
ρ_{FM}	DENFM	Density of the air-propellant mixture $-g/cm^3$
ρ_L	DENL	Liquid density kg/m^3
D_V	DV	Diffusivity of propellant gas across the gas film, cm^2/sec - needed for Schmidt No.
N_{GR}	GR	Grashof Number - $g\beta\Delta t\ L^3\ \rho^2_L\ /\ \mu^2_L$
h	H	Heat transfer rate coefficient, $J/m^2\cdot hr\cdot^{o}K$
C_{PFA}	HCA	Heat capacity of air, $J/g\cdot^{o}K$
h_g	HG	Heat transfer rate coefficient, from the ground to the liquid pool, $J/m^2\cdot hr\cdot^{o}K$
Ω_{A-P}	OMEGA	Collision integral for diffusion, function of kT/ε_{A-P}
P_R	PR	Prandt's number for the vapor phase = $C_{PFM}\ \mu_{FM}/k_{FM}$
N_{PR}	PRL	Prandtl No. for the liquid phase = $\frac{C_L\ \mu_L}{k_L}$
N_{ra}	RA	Rayleigh No. = $N_{GR} * N_{PR}$

LIST OF SYMBOLS (continued)

Computed Variables		Variable Description
Technical Report	Computer Program	
r_{A-P}	RBAR	Average collision diameter of the air propellant molecules, A^{O}
S_C	SC	Schmidt number, dimensionless = $\mu/\rho D_V$
T_A	TA	Temperature of Air, ^{O}C
T_F	TF	Average temperature vapor film, ^{O}C = $(T_P + T_A)/2$
k_{FM}	TCOFM	Thermal conductivity of the propellant-air mixture
k_{FA}	TCONA	Thermal conductivity of air, J/hr·m·^{O}K
k_L	TCONL	Liquid thermal conductivity, J/m·hr·^{O}K
k_{FP}	TCONP	Thermal conductivity of the pure propellant vapor J/hr·m·^{O}K
T_P	TP	Computed temperature of the pool, ^{O}K
-	TPT	Temporary pool temperature calculated by using Raphson-Newton method
$Q_H + Q_G$	TPT_1	Convective heat transfers from (to) the atmosphere + from the soil, J/hr
$Q_E + Q_S +$ $Q_A - H_e$	TPT_2	Radiative heat loss from the liquid pool + CONST J/hr
k_m	TRK	Mass transfer rate coefficient, m/hr
Q_M	VAPRT	Emission rate from the liquid evaporating pool, kg/hr
μ_{FA}	VISA	Viscosity of air, poise = g/cm-sec
μ_{FM}	VISFM	Viscosity of the air-propellant vapor mixture, poise
μ_L	VISL	Liquid viscosity kg/m·hr
μ_{FP}	VISP	Viscosity of the pure gas, component, poise

LIST OF SYMBOLS (continued)

Computed Variables		Variable Description
Technical Report	Computer Program	
V_o	VO	Volume of liquid propellant at its normal boiling point, cc/g-mole
P_v	VPP	Vapor pressure of the pure gas components, $kP_a = kN/m^2$
Y	Y	Average mole fraction of the pure vapor component
r_p	-	Collision diameter of propellant molecules = $1.18\ V_o^{1/3}$ Angstroms
N_{NU}	-	Nusselt Number = $hg\ L/k_L$

LIST OF SYMBOLS

INPUT DATA TO EVAP PROGRAM

Input Symbol		Variable Description
Technical Report	Computer Report	
A_p	ASPILL	Area of Spill
D	DP	Depth of pool in meters
X	DSPILL	Diameter of spill, m
n	GN	Ground roughness factor and temperature profile in the atmosphere
-	KP	Liquid propellant type to be evaluated: KP = 1, 2, 3 1 - N_2H_4 2 - MMH, 3 - UDMH
R_s	RS	Solar insolation rate, $J/m^2 \cdot hr$
T_A	TAC	Temperature of air, ^oC
T_G	TG	Ground temperature at 10 cm depth
$\bar{U}$	$\bar{U}$	Wind speed, m/sec

APPENDIX C

SENSITIVITY ANALYSES

Tables C-1 through C-11 depict input parameter variation and the resulting evaporation rates for the following initial hydrazine spill conditions:

a.	Air temperature	15°C
b.	Wind speed	3 m/sec
c.	Spill volume	20 m^3
d.	Spill diameter	31.66 m
e.	Spill area	787.40 m^2
f.	Ground roughness factor	0.25
g.	Solar rate	3.1(10^6) J/m^2-hr
g.	Solar rate	3.1(10^6) J/m^2·hr
h.	Liquid type	hydrazine
i.	Ground temperature =	air temperature
j.	Depth of pool	2.54 cm

Table C-1 illustrates the variation in evaporation rates between hydrazine, MMH and UDMH. In general, the evaporation rates of UDMH and MMH are 11 and 3 times that of hydrazine. Table C-11 shows that the evaporative heat loss is the major factor reducing the pool temperature. Since the evaporation rate is a function of the vapor pressure of the propellant and the mass transfer coefficient, the mass transfer coefficient must be the factor increasing the evaporation rate while reducing the pool temperature.

Table C-2 indicates that ground temperature is both a high and medium sensitivity input parameter to the evaporation program. When the ground temperature is below the equilibrium pool temperature, heat transfer occurs only by conduction. Table C-2 indicates that a 24 percent error in the evaporation rate occurs for every 10°C error in the ground temperature for the above condition. When ground temperature exceeds the pool temperature, heat transfer usually occurs by turbulent convection. Table C-2 indicates that a 55 percent error can occur for this condition. Table C-11 shows that heat transfer by convection is on the order of 200 percent greater than by conduction.

Evaporation rate is directly proportional to spill area and increases non-linearly with the spill diameter. Table C-3 illustrates the variation in evaporation rate with constant increases in spill diameter. Assuming a 30 meter (diameter) spill, a 33 percent variation in the spill diameter results in a 75 percent overestimate or a 54 percent underestimate in the evaporation rate. This example assumes a 20 m^3 trailer spill.

Table C-4 indicates that an error in the insolation rate can produce a proportional error in the evaporation rate for high insolation values. When the insolating rate is low (compared to the other terms in the heat balance equation), the resultant pool temperature and therefore the evaporation rate is little influenced. Table C-4 shows that for solar insolation below 0.8 $MJ/m^2 \cdot hr$ (late afternoon or early morning), heating effect of the sun is insignicant. When insolation is above 0.8 $MJ/m^2 \cdot hr$ (analysis valid only for the input parameters described above), the heat transfer to the ground or to the air are not sufficient to balance the solar heat input, resulting in a higher pool temperature and increased evaporation rate.

Wind speed is a medium sensitive parameter in the propellant evaporation program. Table C-5 shows that as wind speed increases from one to five meters per second, the evaporation rate doubles. Table C-11 indicates that the primary parameter responsible for the increased evaporation rate is the mass transfer coefficient (km), a function of velocity, which doubles the evaporative heat loss from the pool.

Pool depth has a negligible effect on the evaporation rate. During heat transfer by conduction, when the ground temperature is cooler than the equilibrium pool temperature, a doubling of the pool depth resulted in a 12 percent average increase in the evaporation rate, The increase did not exceed 20 percent for any specific pool depth. During the conductive heat transfer phase, the heat transfer coefficient to the ground reduces to the simple expression:

$$h_g = \frac{k_L}{L}$$

As the pool depth (L) increases, h_g decreases and the pool warms up. During the convective heat transfer phase, h_g is a more complicated function where L is also in the numerator. Thus, when pool temperature is less than the ground temperature, depth is not a sensitive parameter in controlling the evaporation rate. Table C-6 illustrates the increase in pool temperature and evaporation rate when pool temperature is greater than the ground temperature.

The ground roughness factor (n), a highly sensitive parameter, was assumed to equal 0.25 for average atmospheric condition (Reference 3). Variation of the pool evaporation rate with n is shown in Table C-7. In general, a 100 percent change in n results in a 43 percent or greater change in the evaporation rate. As n increases, the velocity term (equation A-4) which is the controlling parameter that affects the evaporation rate, decreases. Although T_p increases, which increases the heat transfer driving force between the air and ground, heat loss to the air is limited by the reduced velocity and heat loss to the ground is a function of the pool depth.

Most attempts to determine the range of n have found that $0<n<1$. The greatest range of observed values is $0.04<n<0.93$ with $n = 0.23$ during conditions of adiabatic lapse rate (Reference 15). This value is very close to the 1/7th power law familiar in turbulent pipe flow (Reference 15). Table C-8 presents values of n for various temperature difference data in the atmosphere between 5 and 400 feet above the ground (Reference 15).

The emissivity of the atmosphere (e_a) is a function of the water vapor pressure in the atmosphere and assumed as 0.75 in this report. Table C-9 shows that e_a is not important in controlling the evaporation rate. A reduction in e_a of 0.25 (33 percent) results in a 10 percent reduction in the evaporation rate.

Variation in air temperature from 0 to 40°C results in a 100 percent increase in the evaporation rate. In general, a 10°C error in the air temperature results in a 20 percent error in the evaporation rate. This variable is designated as a medium sensitive parameter. Table C-10 shows the variation of evaporation rate with increasing air temperature.

TABLE C-1. VARIATION OF EVAPORATION RATE WITH PROPELLANT

Propellant	Pool Temperature	Evaporation Rate
	^{o}K	kg/hr
Hydrazine	299.2	538.5
MMH	293.2	1704
UDMH	287.7	5807

TABLE 2-C. VARIATION OF EVAPORATION RATE WITH GROUND TEMPERATURE

Ground Temperature	Pool Temperature	Evaporation Rate
^{o}K	^{o}K	kg/hr
273	293.3	385.7
283	297.3	483.8
293	301.1	597.8
303	304.7	727.0
313	312.8	1111.5
318	317.7	1426.4

TABLE C-3. VARIATION OF EVAPORATION WITH SPILL SIZE

Spill Diameter	Spill Area	Pool Temperature	Evaporation Rate
m	m^2	^oK	kg/hr
10	78.5	298.3	57.8
20	314.2	298.9	221
30	706.9	299.2	485
40	1256.6	299.5	848
50	1963.45	299.7	1306

TABLE C-4. VARIATION OF EVAPORATION RATE WITH SOLAR INSOLATION

Solar Insolation	Pool Temperature	Evaporation Rate
MJ/m^2hr	^oK	kg/hr
0.1	288	283
0.2	288	283
0.4	288	283
0.8	288	283
1.6	292	358
3.2	300	569
6.4	314	1186

TABLE C-5. VARIATION OF EVAPORATION RATE WITH WIND SPEED

Wind Speed m/sec	Pool Temperature ^{o}K	Evaporation Rate Rate kg/hr
1	305	319
2	302	448
3	299	539
4	298	612
5	296	674

TABLE C-6. VARIATION OF EVAPORATION RATE WITH POOL DEPTH

Pool Depth Centimeters	Pool Temperature ^{o}K	Evaporation Rate kg/hr
0.15875	290	309
0.3175	291	335
0.635	293	381
1.27	296	451
2.54	299	538
5.08	302	622
10.16	304	683
20.32	305	721

TABLE C-7. VARIATION OF EVAPORATION RATE WITH THE GROUND ROUGHNESS FACTOR

Ground Roughness Factor (n)	Pool Temperature °K	Evaporation Rate kg/hr
0.1	289.1	1220
0.2	295.8	693
0.3	302.4	419
0.4	307.4	247
0.5	310.6	140
0.6	312.4	78
0.7	313.4	44
0.8	313.9	25
0.9	314.2	15
1.0	314.2	9

TABLE C-8. VALUES OF GROUND ROUGHNESS FACTOR RELATED TO THE TEMPERATURE DIFFERENCE

$\Delta T = T_{400} - T_5$ in the LAYER 5-400 Feet

$\Delta T, {}^{o}C$	-2.2 to -1.1	-1.4 to -0.8	-1.1 to 0	-0.6 to +0.6	0 to 1.1	1.1 to 2.2	2.2 to 3.3	3.3 to 4.4	4.4 to 5.6	5.6 to 6.7
n	0.25	0.29	0.40	0.45	0.49	0.61	0.74	0.77	0.77	0.87

TABLE C-9. VARIATION OF EVAPORATION RATE WITH ATMOSPHERIC EMISSIVITY

Emissivity	Pool Temperature ^{o}K	Evaporation Rate kg/hr
0.75	299.2	539
0.65	298.5	516
0.55	297.7	494
0.45	296.6	473
0.35	296.1	452

TABLE C-10. VARIATION OF EVAPORATION RATE WITH AMBIENT AIR TEMPERATURE

Air Temperature ^{o}K	Pool Temperature ^{o}K	Evaporation Rate kg/hr
273	294.3	408
283	297.7	493
293	300.8	588
303	303.9	695
313	306.9	818

TABLE C-11. HEAT TRANSFER SENSITIVITY ANALYSIS

Independent Variable	Heat Transfer Parameters (hundred megacal/hr) Q_a $\epsilon_p \sigma T_a^4 A_p$	Q_s $(1-a) R_s A_p$	Q_h $h (T_a - T_p) A_p$	Q_G $h_G (T_G - T_p) A_p$	Q_e $\epsilon_p \sigma T_p^4 A_p$	H_e $k_m A_p M_w \lambda_p P_v / RT$	Computed Variables T_p	Evap
KP = 1	1.98	5.08	-0.91	-1.48	-2.93	-1.74	299	538
KP = 2	1.98	5.08	-0.43	-0.35	-2.70	-3.58	293	1704
	0	0	0.48/53%	1.13/76%	.23/8%	1.84/106%	6/2%	116/217%
KP = 1	1.98	5.08	-0.91	-1.48	-2.93	-1.74	299	538
KP = 3	1.98	5.08	0.03	3.64	-2.50	-8.23	288	5807
Diff/% Var	0	0	0.94/103%	5.12/346%	.43/15%	6.49/373%	11/4%	5269/980%

The evaporative heat loss is the major driving force lowering the equilibrium pool temperature. Although the reduction in the pool temperature lowers the vapor pressure, the larger mass transfer rate coefficient more than compensates for this.

T_C = 273	1.98	5.08	-0.44	-2.67	-2.70	-1.26	293	386
T_G = 303 / 45°C	1.98	5.08	-1.34	-0.24	-3.15	-2.34	305	727
	0/0	0/0	0.90/205%	2.43/91%	0.45/17%	1.08/86%	12/4%	341/88%
T_G = 303	1.98	5.08	-1.34	-0.24	-3.15	-2.34	305	727
T_G = 318 / 15	1.98	5.08	-2.36	3.54	-3.72	-4.52	317.7	1426
	0	0	1.02/76%	3.78/1575%	0.57/18%	2.18/93%	12.7/4%	699/96%

In the above example, $T_p > T_G$ and conductive heat transfer occurs. Below, $T_G > T_p$ and heat transfer into the pool occurs by turbulent convection. During conduction, a 10°C increase in T_G results in an average 24 percent increase in the evaporation rate. During turbulent convection, a 10°C increase in T_G results in a 55 percent increase in evaporation.

TABLE C-11. HEAT TRANSFER SENSITIVITY ANALYSIS

Independent Variable	Heat Transfer Parameters (hundred megacal/hr)						Computed Variables	
	Q_a $e_a s T_A^4 A_p$	Q_s $(1-a) R_s A_p$	Q_h $h (T_A - T_p) A_p$	Q_G $bg (T_G - T_p) A_p$	Q_e $e_p s T_p^4 A_p$	H_e $km A_p MW \lambda_p P_V$ / RT	T_p	Evap
A_p = 587.4 A_p = 1087.4	1.48 2.74 1.26/85%	3.79 7.01 3.22/85%	-0.68 -1.25 0.57/85%	-1.11 -2.05 0.94/85%	-2.19 -4.05 1.86/85%	-1.30 -2.41 1.11/85%	299 299 0	402 744 324/85
A variation in the spill area results in a proportionate change in the evaporation rate. Since all heat transfer terms are equally affected, a net change in the pool temperature does not result.								
R_s = 12,500 R_s = 200,000	1.98 1.98 0	0.08 1.35 1.27/1590%	0.006 0.0004 0.0056/93%	1.36 0.10 1.26/93%	-2.51 -2.51 0	-0.93 -0.93 0	287.9 287.9 0	283 283 0
R_s = 200,000 R_s = 800,000	1.98 1.98 0	1.35 5.42 4.07/300%	0.0004 -0.98 0.98/2450%	0.10 -1.61 1.71/1710%	-2.51 -2.97 .46	-0.93 -1.84 .91/100%	287.9 300	283 569 286/100%
Solar insolation below 200,000 cal/m^2-hr, occurring approximately one to two hours after sunrise or before sunset (clear sky) does not affect the net heat balance, and therefore the pool temperature or evaporation rate. When R varies from 200,000 to 800,000 cal/m^2-hr, the evaporation doubles.								
U = 1 U = 5	1.98 1.98 0	5.08 5.08 0	- .59 - .98 .39/66%	-2.27 -1.08 1.19/52%	-3.17 -2.81 .36/11%	-1.02 -2.19 1.17/115%	305 296 9/3%	319 674 355/111%
Increasing wind speed results in higher evaporative heat loss, reduced pool temperature and increased mass transfer rate. An increase in wind speed from one to five meters per second doubles the evaporation rate.								

TABLE C-11. HEAT TRANSFER SENSITIVITY ANALYSIS

Independent Variable	Heat Transfer Parameters (hundred megacal/hr) Q_a $\epsilon_a \sigma T_A^4 A_p$	Q_s $(1-a) R_s A_p$	Q_c $h (T_A - T_p) A_p$	Q_G $h_g (T_G - T_p) A_p$	Q_e $p^* T_p^4 A_p$	H_e $\frac{k_m A_p M_W \lambda_p P_w}{RT}$	Computed Variables T_p	Evap
DP = .001587	1.98	5.08	.13	-3.35	-2.57	-1.01	289.5	309
DP = .2032	1.98	5.08	-1.33	-0.27	-3.14	-2.32	304.6	721
	0	0	1.20/92%	3.08/92%	0.57/22%	1.31/130%	15.1/5%	412/133%

The percent variation of evaporation with depth depends on the heat transfer mechanisms. For conduction, $H_e = k_t/L$ and the pool temperature and the evaporation rate increase with increasing L. In general, for spill depths of 1/16 inch to 8 inches, a doubling of L results in a 10 percent average increase in evaporation rate. For turbulent convective heat transfer, L is both in the numerator and denominator of the heat transfer equation. The effect of L on the heat transfer rate coefficient is negligible.

n = 0.1	1.98	5.08	-0.37	-0.15	-2.55	-3.99	289	1220
n = 0.5	1.98	5.08	-0.25	-2.96	-3.40	-0.45	311	140
	0	0	0.12/32%	2.81/1870%	.85/33%	3.54/89%	22/8%	1080/89%

n is assumed to be equal to 0.25 for average atmospheric conditions. A variation of n from 0.2 to 0.1 and 0.3 results respectively in a 76% and 40% variation in the evaporation rate.

TABLE C-11. HEAT TRANSFER SENSITIVITY ANALYSIS

Independent Variables	Heat Transfer Parameters (hundred megacal/hr) Q_a $e_a \sigma T_A^4 A_p$	Q_s $(1-a) R_s A_p$	Q_h $h (T_A - T_p) A_p$	Q_c $k_g (T_c - T_p) A_p$	Q_e $e_p \sigma T_p^4 A_p$	H_e $\frac{k_m A_p M W \lambda_p P_v}{RT}$	Computed Variables T_p	Evap
e_a = 0.45	1.19	5.08	-0.72	-1.18	-2.84	-1.53	297	473
e_a = 0.75	1.98	5.08	-0.91	-1.48	-2.93	-1.74	299	538
	0.79/66%	0	0.19/26%	0.30/25%	0.09/3%	0.21/14%	2/1%	65/14%
T_A = 273	1.60	5.08	-1.77	-0.843	-2.74	-1.33	294	408
T_A = 313	2.76	5.08	+0.47	-2.46	-3.23	-2.63	307	818
45	1.16/73%	0/0	2.14/121%	1.62/193%	0.49/18%	1.30/98%	13/4.8%	410/100%

Variation of the emissivity by 67% results in a 14% change in the evaporation rate. In general, doubline e_a results in a 16% increase in the evaporation rate.

As T_A increases from 0 to 40°C, the equilibrium pool temperature increases by 13°C and the evaporation rate doubles.

INITIAL DISTRIBUTION

HQ USAF/LEEVP	2	Det 1 ADTC/TST (Tech Library)	1
HQ USAF/SAFOI	1	Det 1 ADTC/ECC	2
HQ USAF/SGPA	1	SAMTEC/WE	1
HQ ADCOM/SGPAP	1	DARCOM, Field Safety Activity	1
NCEL, Code 25111	1	Southeast Envmtl Rsch Lab	1
HQ TAC/SGPB	3	DD-MED-41	1
HQ USAFE/Surgeon	1	AFOSR/NC	1
HQ USAFE/DEPV	1	AWS/DNP	1
HQ AFISC/SGMS	1	HQ SAC/DOW	1
HQ USAFA/DEV	1	AFRPL/WE	1
Toxic Materials Info Ctr	1	Det 1 ADTC/DAY	2
AFOSR/Life Sciences	1	HQ AFSC/DLCA	2
AMRL/THE	3	SAF/MIQ	1
SAMSO/DEV	1	AFIT/DE	1
HQ AFSC/DEV	1	USN Chief, R&D/EQ	1
HQ AFSC/SGPE	1	1 MSEW	1
HQ ATC/SGPAP	1	6595 STESTG/TS	1
HQ MAC/SGPE	1	USAF Hospital/SGPB	1
HQ PACAF/SGPE	1	DOD Explosives Safety Board	1
HQ SAC/SPGA	1	SAMSO/WE	1
Cmdr, US Army Med Bioengrg Lab	1	SAMTEC/WE	1
OEHL/CC	3	OEHL	1
AFWL/SUL	1	AFWL/WE	1
AFGL/XOP	1	HQ AFSC/SD	1
USAFSAM/EDE	2	AFIT/Library	1
AFRPL/Library	1	Federal Laboratory Program	1
SAMTEC/SEH	1	USA Chief, R&D/EQ	1
OEHL	1	HQ AU/AUL	1
SAMSO/SG	1	HQ USAFA/Library	1
AMD/RDU	1	HQ AFTEC/SG	1
ADTC/CSV	1	HQ AFSC/SOSM	1
AFETR/DER	1	EPA/ORD	1
OASD/(MRA&L)ES	1	HQ NASA (MHS-7)	1
Det 1 ADTC/CC	1	HQ AFISC/SES	2
AFCEC/SU	1	USAF Hospital/SGP, Eglin AFB	1
Det 1 ADTC/WE	2	1 STRAD/SEM	1
AFCEC/DEV	1	USAF Hospital/SGP, Edwards AFB	1
Det 1 ADTC/ECA	5	6595 STESTG/SZ	1
Det 1 ADTC/ECW	3	SAI	1
AFTAC/TRA	1	Det 1 ADTC/EC	1
Dir/CC Chem Sys Lab	3		
OG-ALC/SGP	1		
USAF Hospital/SGPM	1		
DDC/TCA	2		
ARPA	1		
Defense Rsch & Engrg/AD	1		
USA Envmtl Hygn Agency	1		